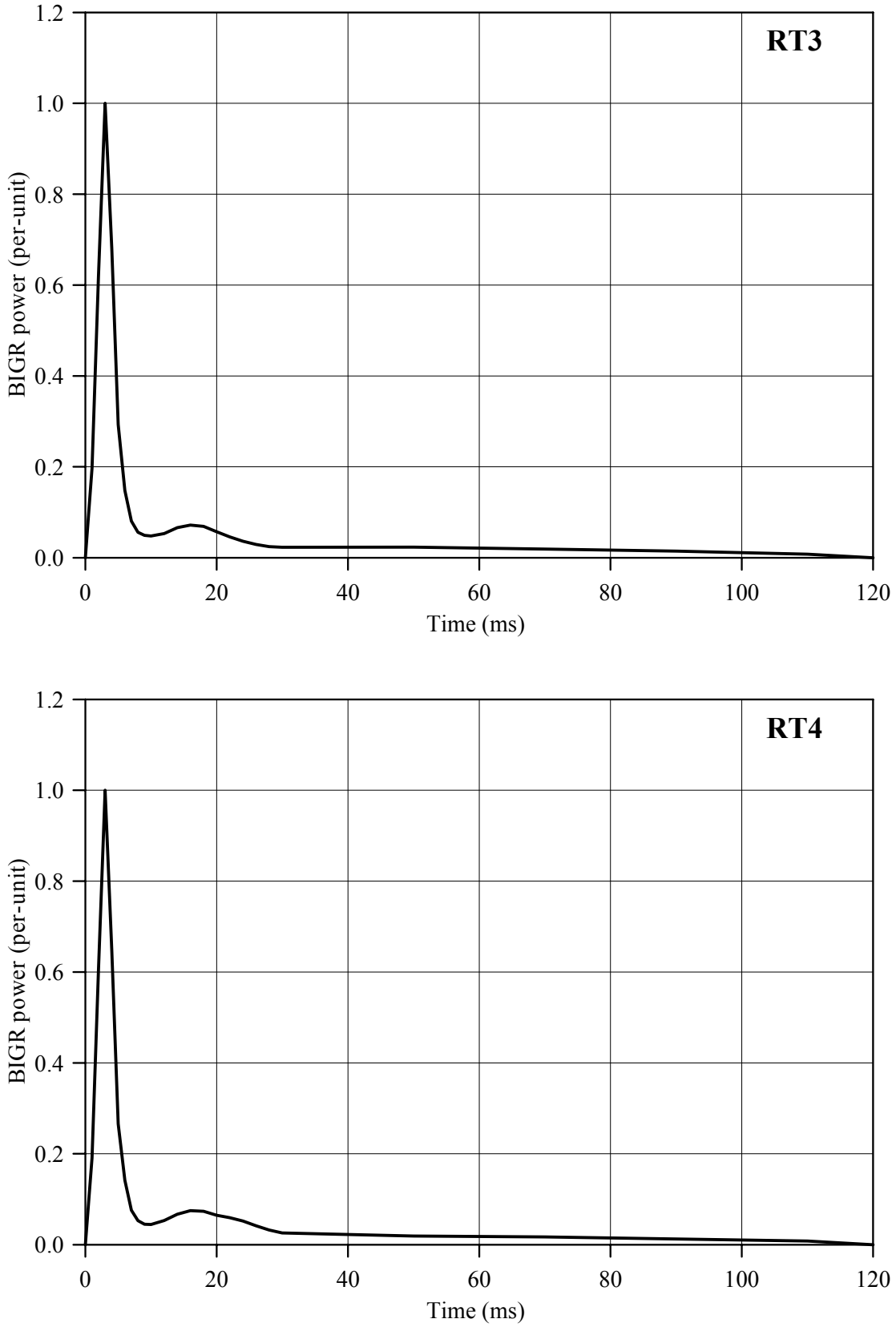


**Fig. D.2. BIGR power for fuel rods # RT3 and # RT4**

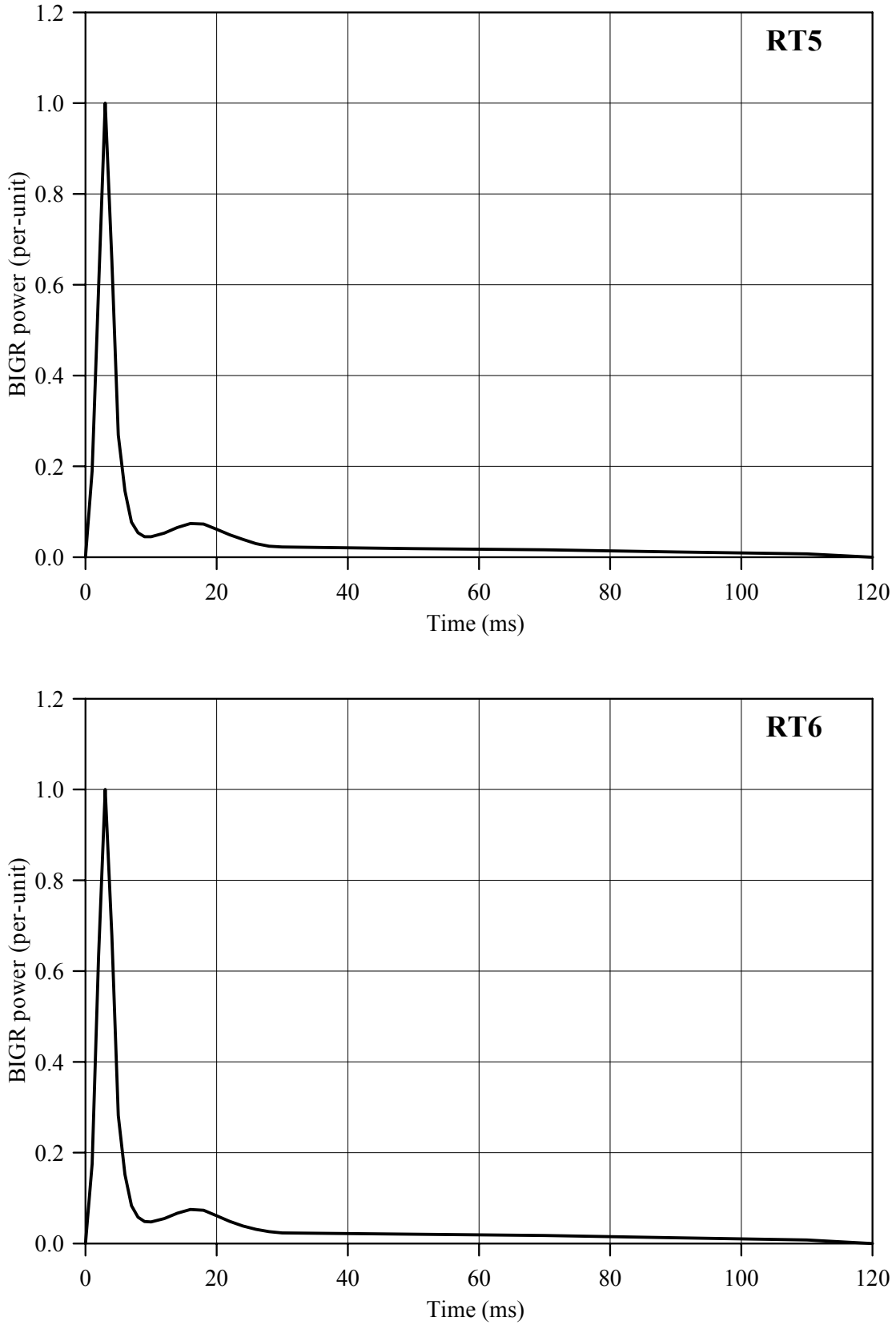


**Fig. D.3. BIGR power for fuel rods # RT5 and # RT6**

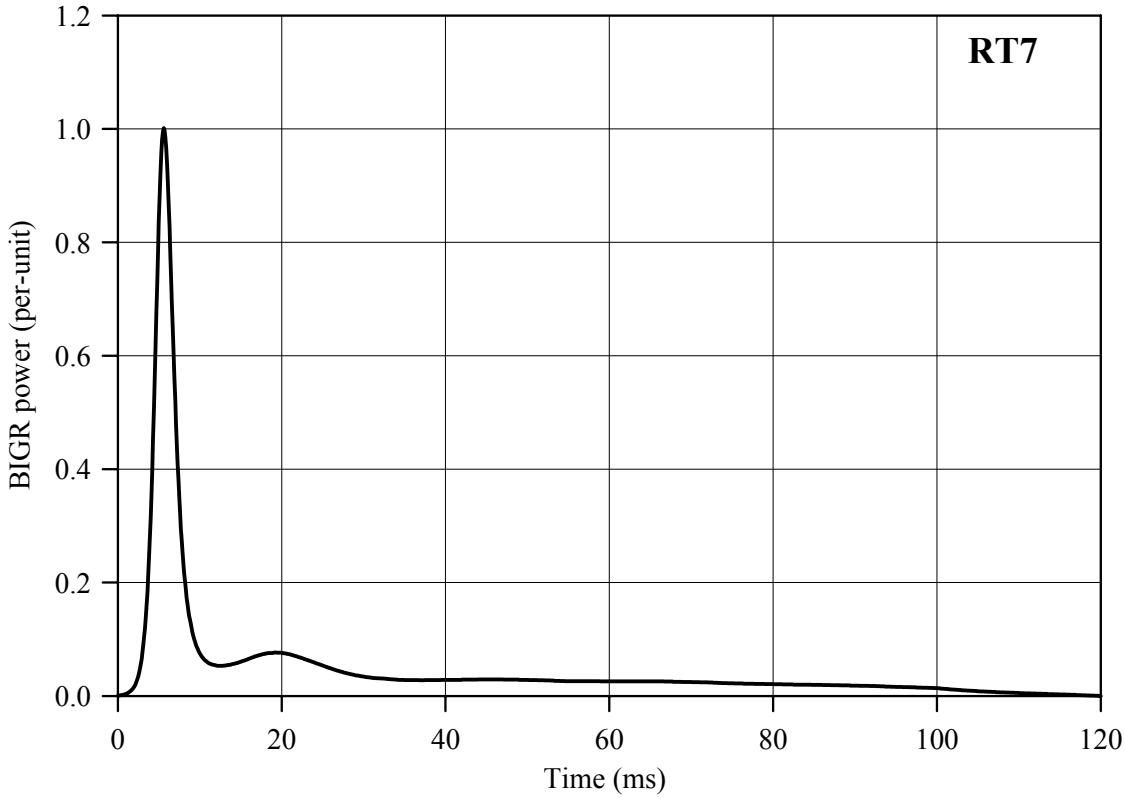


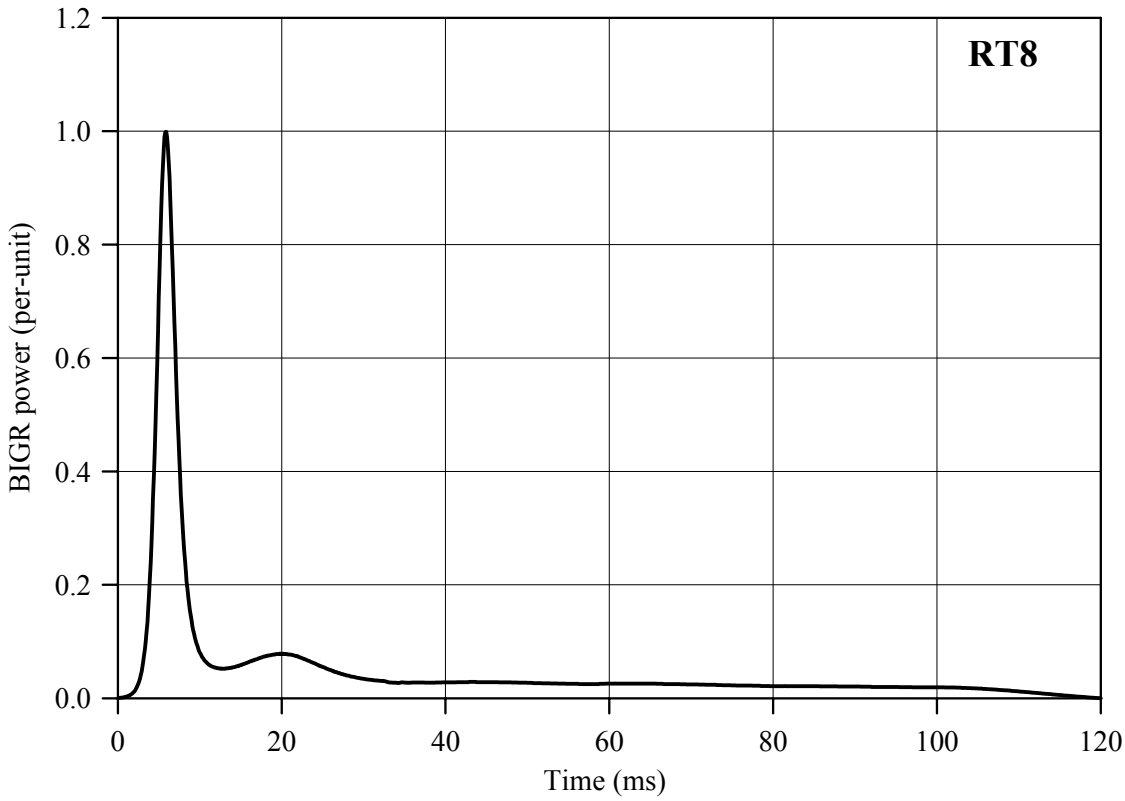


**Fig. D.4. BIGR power for fuel rods # RT7 and # RT8**

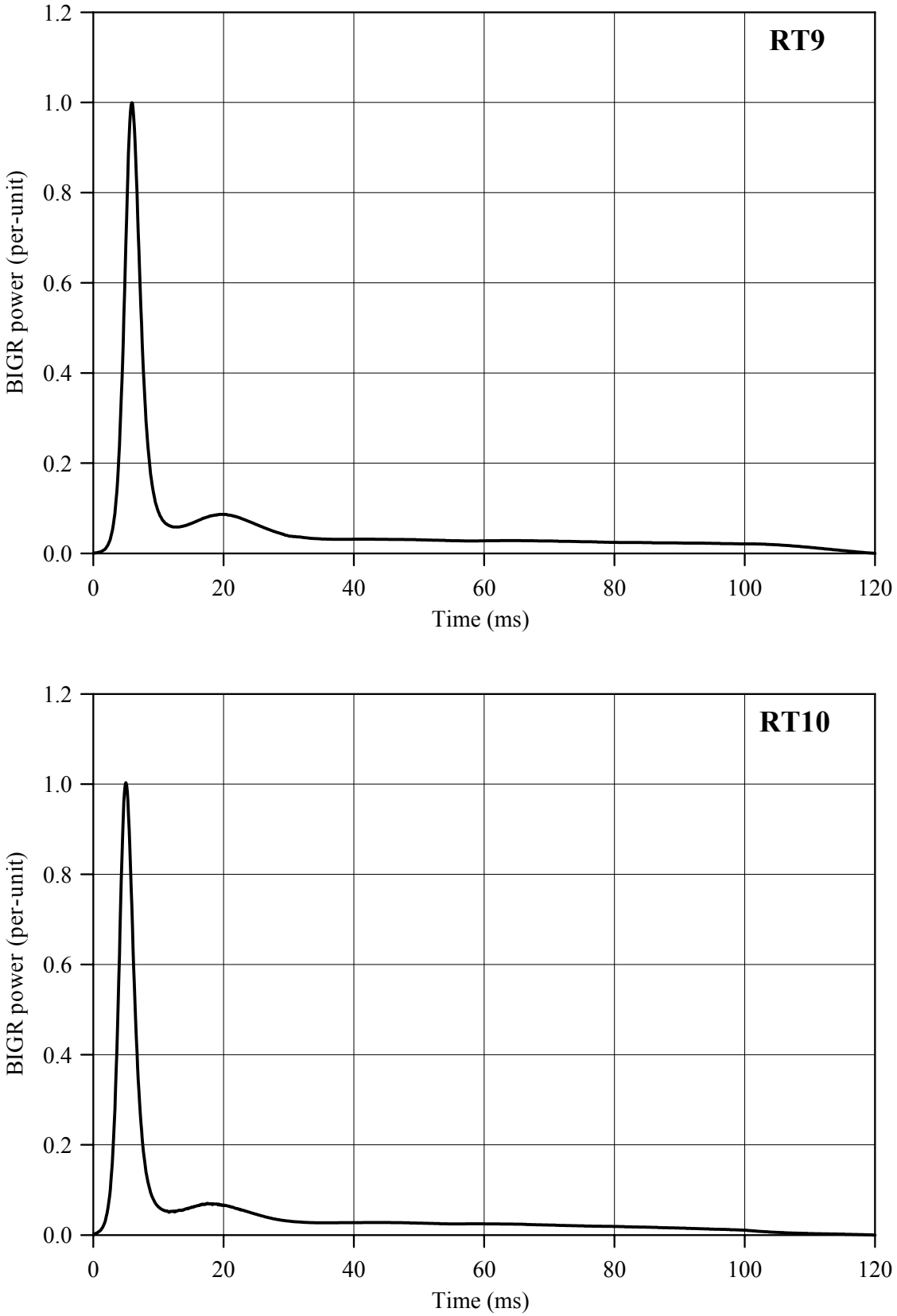


**Fig. D.5. BIGR power for fuel rods # RT9 and # RT10**

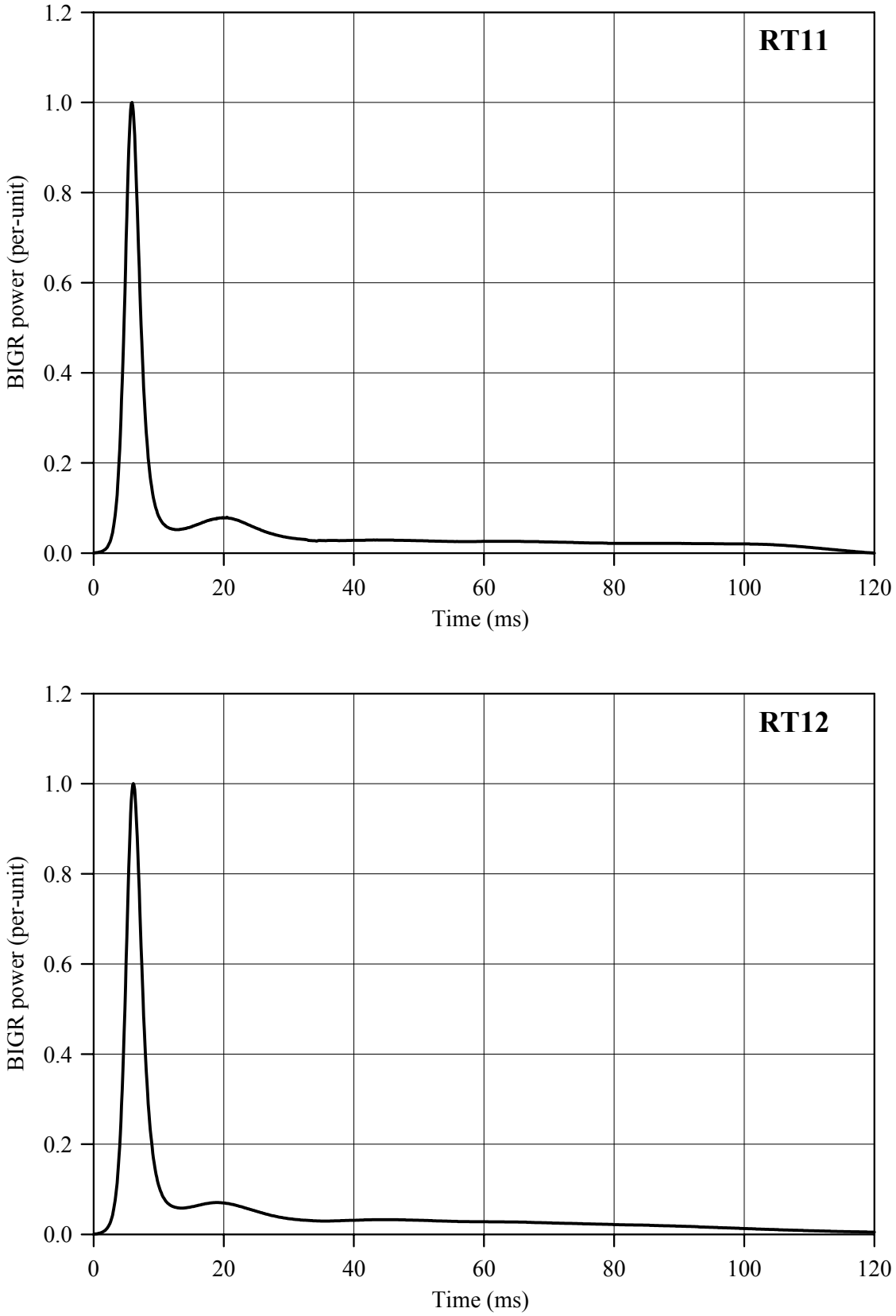


**Fig. D.6. BIGR power for fuel rods # RT11 and # RT12**

# APPENDIX E

# CHARACTERISTICS OF REFABRICATED FUEL RODS AFTER THE BIGR TESTS

## *Appendix E–1*

## *Individual Characteristics of Fuel Rod # RT1 after the BIGR Test*

# # RT1

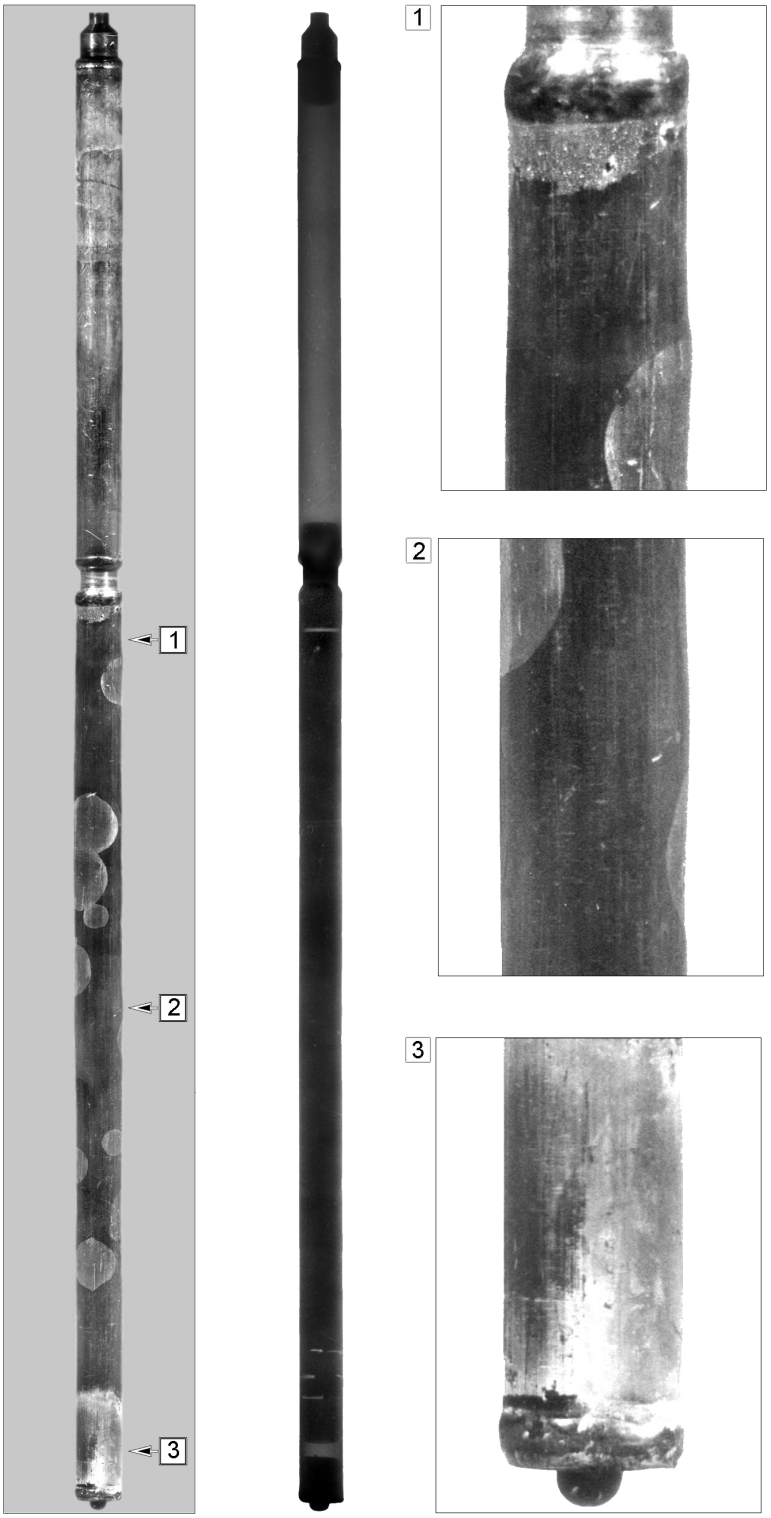


**Fig.E-1.1. Appearance of unfailed fuel rod # RT1 after the BIGR test (photographs and X-ray photograph)**

# # RT1

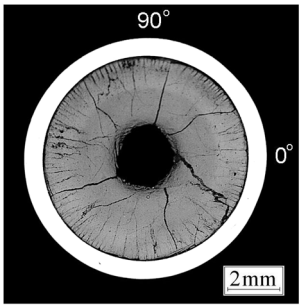


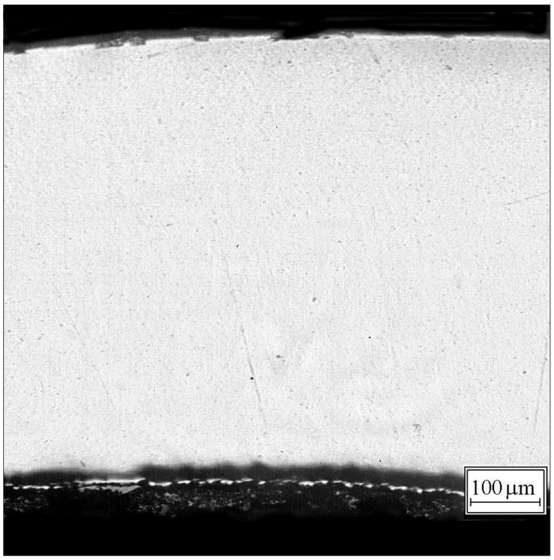


**Fig.E-1.2. Cross-section and cladding microstructure of fuel rod # RT1 at 113 mm elevation (from low cap)**

# # RT1

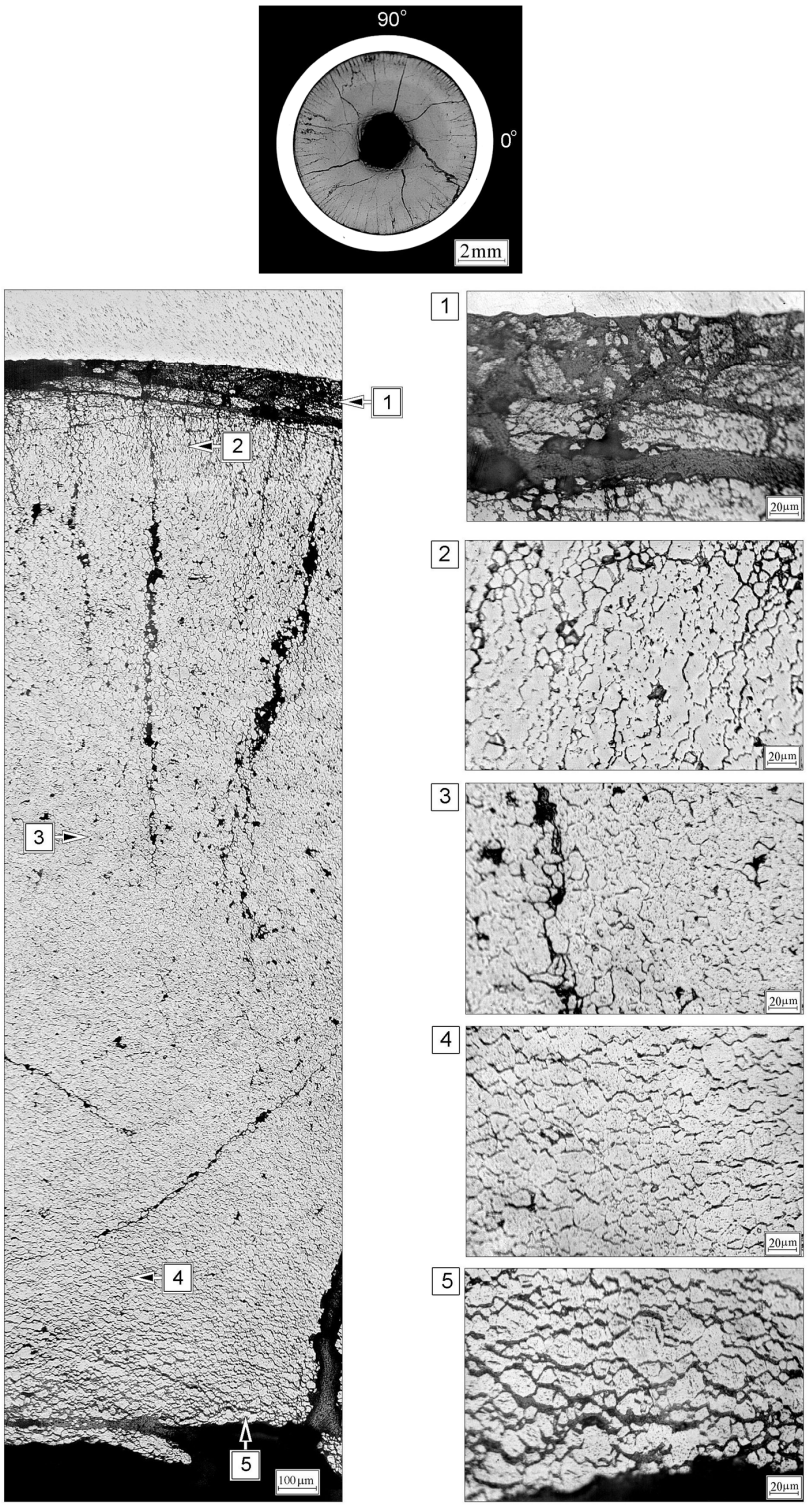


**Fig.E-1.3. Cross-section and fuel microstructure of fuel rod # RT1 at 113 mm elevation (from low cap)**

**Table E-1.1. Time dependent energy characteristics of fuel rod # RT1**

| Time (s) | Relative reactor power (current/ maximum value) (per-unit) | Cumulative number of fissions in fuel rod (fiss) x$10^{-14}$ | Power of fuel rod[1)2)] (kW) | Energy deposition | | Fuel enthalpy[3)] | |
|---|---|---|---|---|---|---|---|
| | | | | (cal/g fuel) | (J/g fuel) | FRAP-T6 | RAPTA-5 |
| 0.000 | 0.00E+00 | 0.000 | 0.000 | 0.000 | 0.000 | 0.000 | 0.000 |
| 0.001 | 1.76E-01 | 0.240 | 1260 | 2.507 | 10.49 | 3.010 | 2.386 |
| 0.002 | 5.73E-01 | 1.166 | 4095 | 12.13 | 50.79 | 13.201 | 12.045 |
| 0.003 | 9.88E-01 | 3.301 | 7069 | 34.44 | 144.2 | 35.610 | 34.383 |
| 0.004 | 7.32E-01 | 5.690 | 5233 | 59.33 | 248.4 | 60.455 | 59.119 |
| 0.005 | 3.19E-01 | 7.017 | 2281 | 73.16 | 306.3 | 74.106 | 72.559 |
| 0.006 | 1.65E-01 | 7.630 | 1181 | 79.57 | 333.1 | 80.313 | 78.541 |
| 0.007 | 8.90E-02 | 7.949 | 636.8 | 82.88 | 347.0 | 83.360 | 81.459 |
| 0.008 | 5.88E-02 | 8.138 | 420.7 | 84.84 | 355.2 | 85.045 | 83.077 |
| 0.009 | 5.24E-02 | 8.284 | 374.5 | 86.33 | 361.4 | 86.262 | 84.264 |
| 0.010 | 5.00E-02 | 8.416 | 357.7 | 87.72 | 367.3 | 87.385 | 85.379 |
| 0.012 | 5.93E-02 | 8.691 | 424.0 | 90.65 | 379.5 | 89.796 | 87.862 |
| 0.014 | 7.33E-02 | 9.037 | 524.4 | 94.22 | 394.5 | 92.851 | 90.944 |
| 0.016 | 8.05E-02 | 9.446 | 575.8 | 98.50 | 412.4 | 96.592 | 94.697 |
| 0.018 | 7.95E-02 | 9.869 | 568.9 | 102.9 | 430.8 | 100.483 | 98.676 |
| 0.020 | 6.85E-02 | 10.26 | 490.0 | 107.0 | 447.9 | 104.037 | 102.320 |
| 0.022 | 5.38E-02 | 10.58 | 384.7 | 110.3 | 461.9 | 106.885 | 105.220 |
| 0.024 | 4.21E-02 | 10.83 | 301.4 | 112.9 | 472.9 | 109.026 | 107.410 |
| 0.026 | 3.29E-02 | 11.03 | 235.3 | 115.0 | 481.4 | 110.633 | 109.200 |
| 0.028 | 2.76E-02 | 11.18 | 197.8 | 116.6 | 488.1 | 111.865 | 110.410 |
| 0.030 | 2.55E-02 | 11.32 | 182.3 | 118.0 | 494.2 | 112.927 | 111.370 |
| 0.050 | 2.33E-02 | 12.59 | 166.4 | 131.3 | 549.7 | 122.572 | 121.330 |
| 0.070 | 1.84E-02 | 13.68 | 131.8 | 142.7 | 597.5 | 130.730 | 129.710 |
| 0.090 | 1.43E-02 | 14.54 | 102.6 | 151.6 | 634.7 | 136.829 | 135.920 |
| 0.110 | 9.12E-03 | 15.17 | 65.43 | 158.2 | 662.5 | 141.113 | 140.300 |
| 0.130 | 3.38E-03 | 15.48 | 24.39 | 161.4 | 675.7 | 142.614 | 141.550 |
| 0.150 | 1.29E-03 | 15.59 | 9.439 | 162.6 | 680.7 | 142.832 | 141.070 |
| 0.200 | 3.45E-04 | 15.68 | 2.730 | 163.6 | 684.8 | 141.257 | 138.770 |
| 1.000 | 3.11E-05 | 15.81 | 0.341 | 165.4 | 692.3 | 121.068 | 117.990 |
| 10.00 | 3.60E-06 | 16.04 | 0.050 | 169.5 | 709.7 | 29.703 | 27.267 |
| 100.0 | 7.01E-08 | 16.15 | 0.008 | 172.5 | 722.4 | 5.033 | 4.508 |
| 1000 | 2.74E-13 | 16.16 | 1.73E-04 | 174.0 | 728.5 | 0.000 | 0.000 |

[1)] Average values determined in accordance with results of RRC KI and VNIIEF calculations

[2)] Maximum power value is 7152.5 kW (t=0.0032 s)

[3)] Average radial value

# # RT1

**Table E-1.2. Radial energy characteristics of fuel rod # RT1***

| Parameters | Coordinates of fuel radial layers (mm) | | | |
|---|---|---|---|---|
| | 1 layer (1.23-2.82) | 2 layer (2.82-3.44) | 3 layer (3.44-3.71) | 4 layer (3.71-3.795) |
| Number of fissions $x10^{-14}$ (fiss) | 7.266 | 4.700 | 2.829 | 1.364 |
| Fission density $x10^{-13}$ (fiss/g fuel) | 2.292 | 2.431 | 2.997 | 4.417 |
| Power** (kW) | 3173 | 2086 | 1264 | 629.7 |
| Energy deposition (cal/g fuel) | 156.6 | 166.5 | 205.1 | 303.3 |
| Energy deposition (J/g fuel) | 655.8 | 697.3 | 858.9 | 1270 |
| Energy deposition*** (per-unit) | 0.517 | 0.550 | 0.677 | 1.000 |

* Average values were determined in accordance with results of RRC KI and VNIIEF calculations

** The power for the entire length of each layer at time 0.0032 s

*** Energy deposition in current layer/energy deposition in $4^{th}$ layer

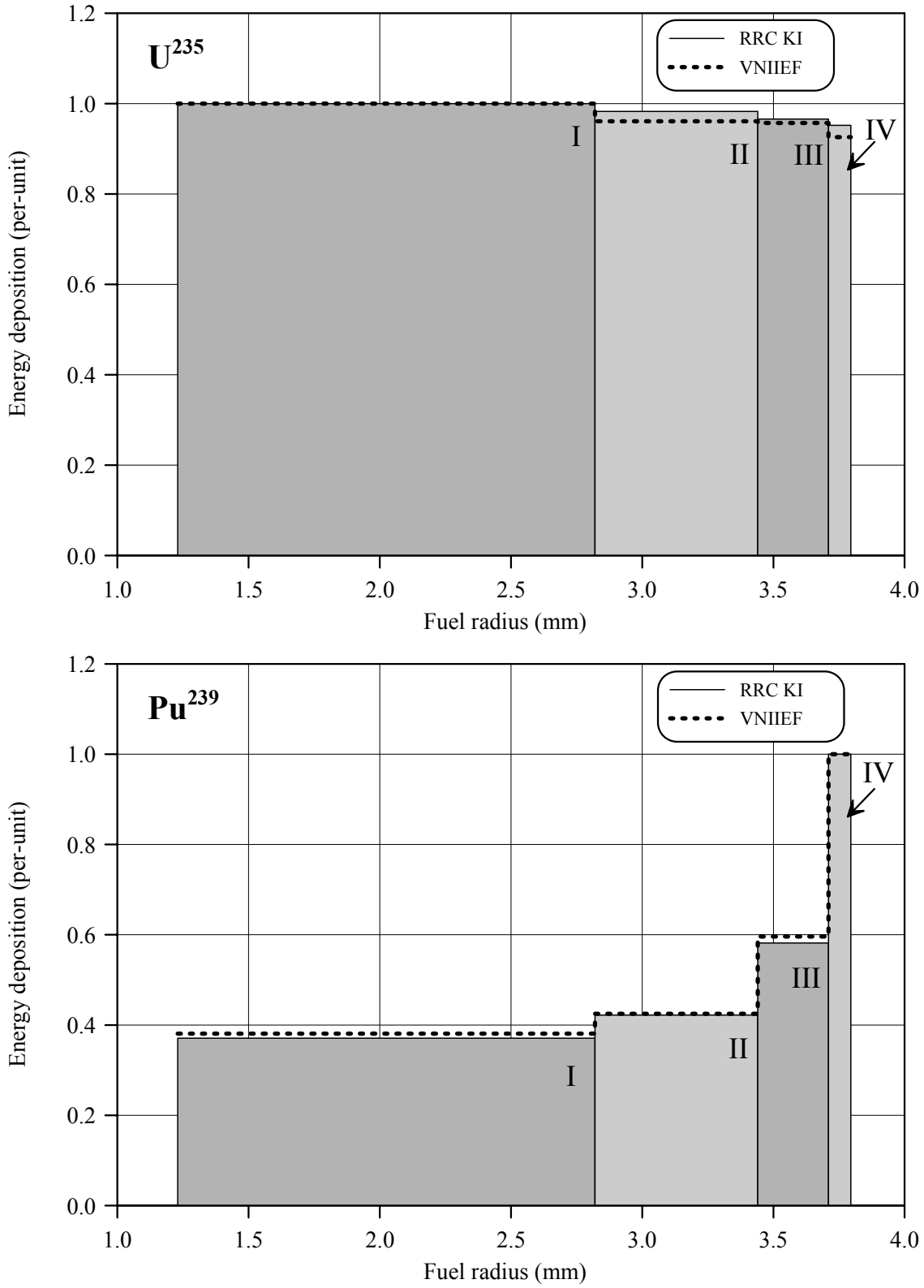


**Fig.E-1.4. $U^{235}$ and $Pu^{239}$ radial distribution of energy deposition for fuel rod # RT1**

# # RT1

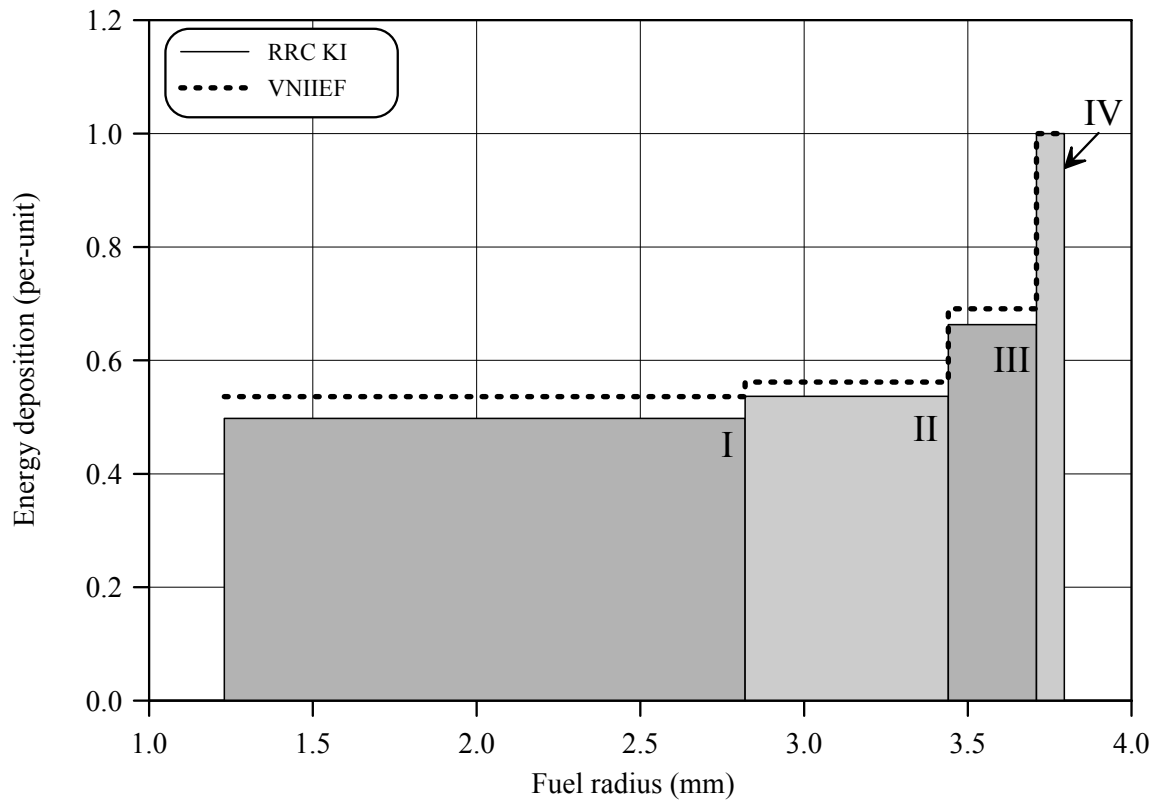


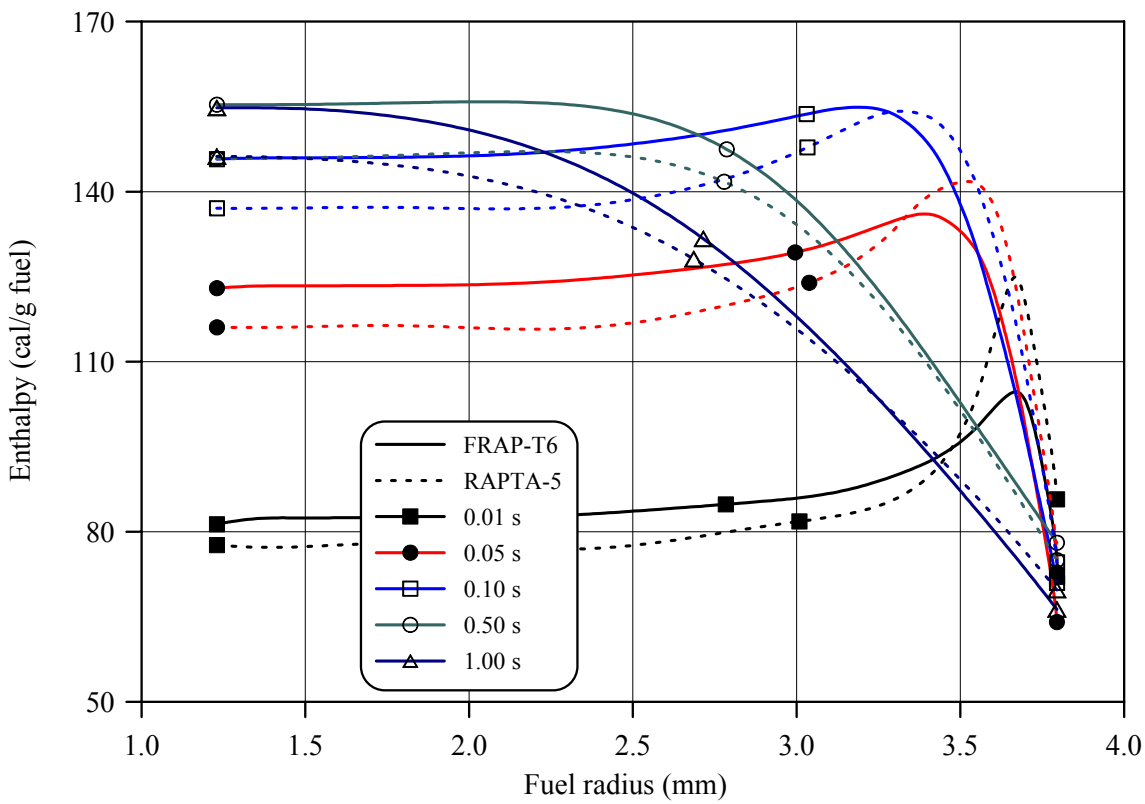


**Fig.E-1.5. Radial distribution of energy deposition and fuel enthalpy for fuel rod # RT1**

# # RT1

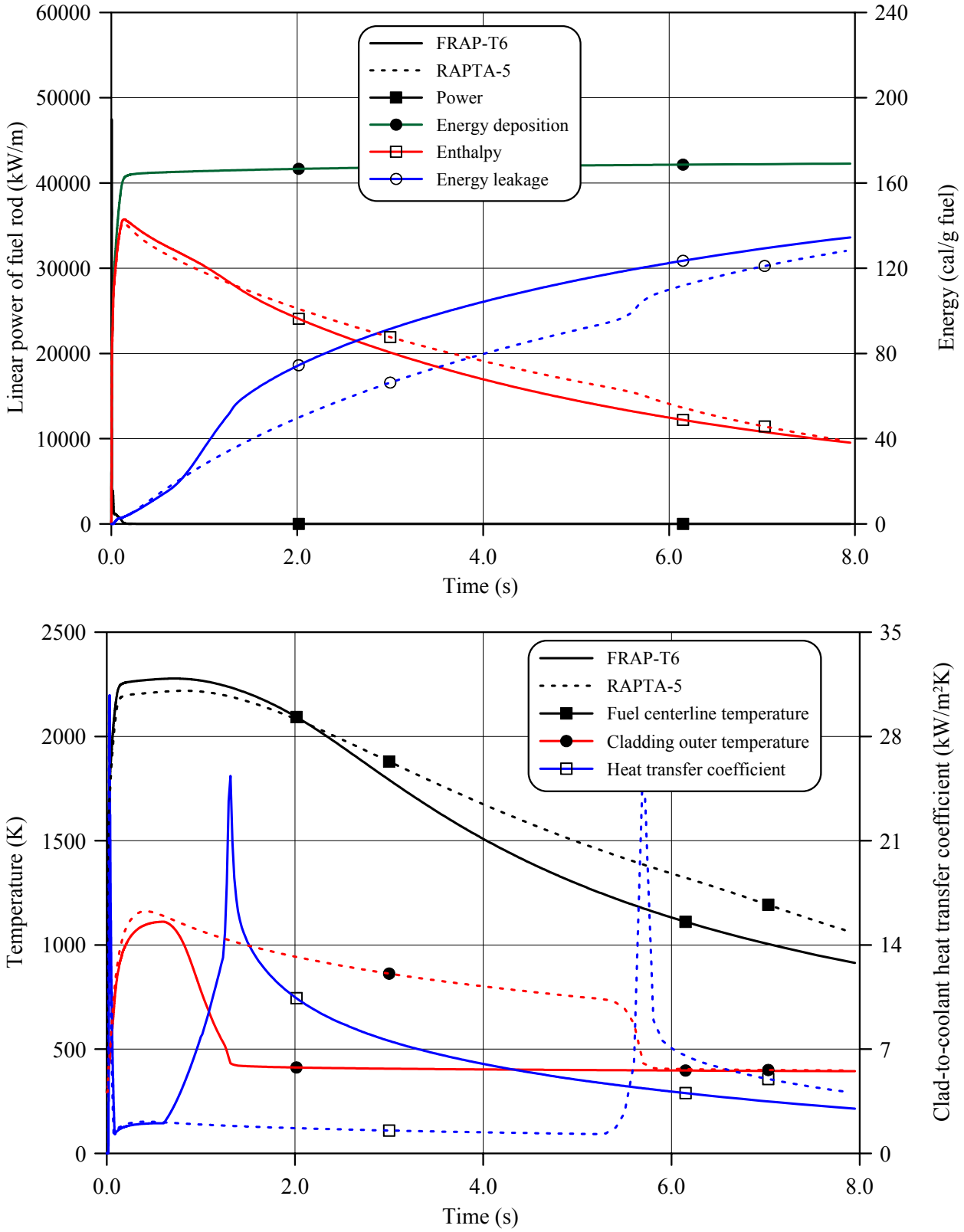


**Fig.E-1.6. Thermal history of fuel rod # RT1 during the BIGR test in accordance with FRAP-T6/VVER and RAPTA-5 calculations**

# # RT1

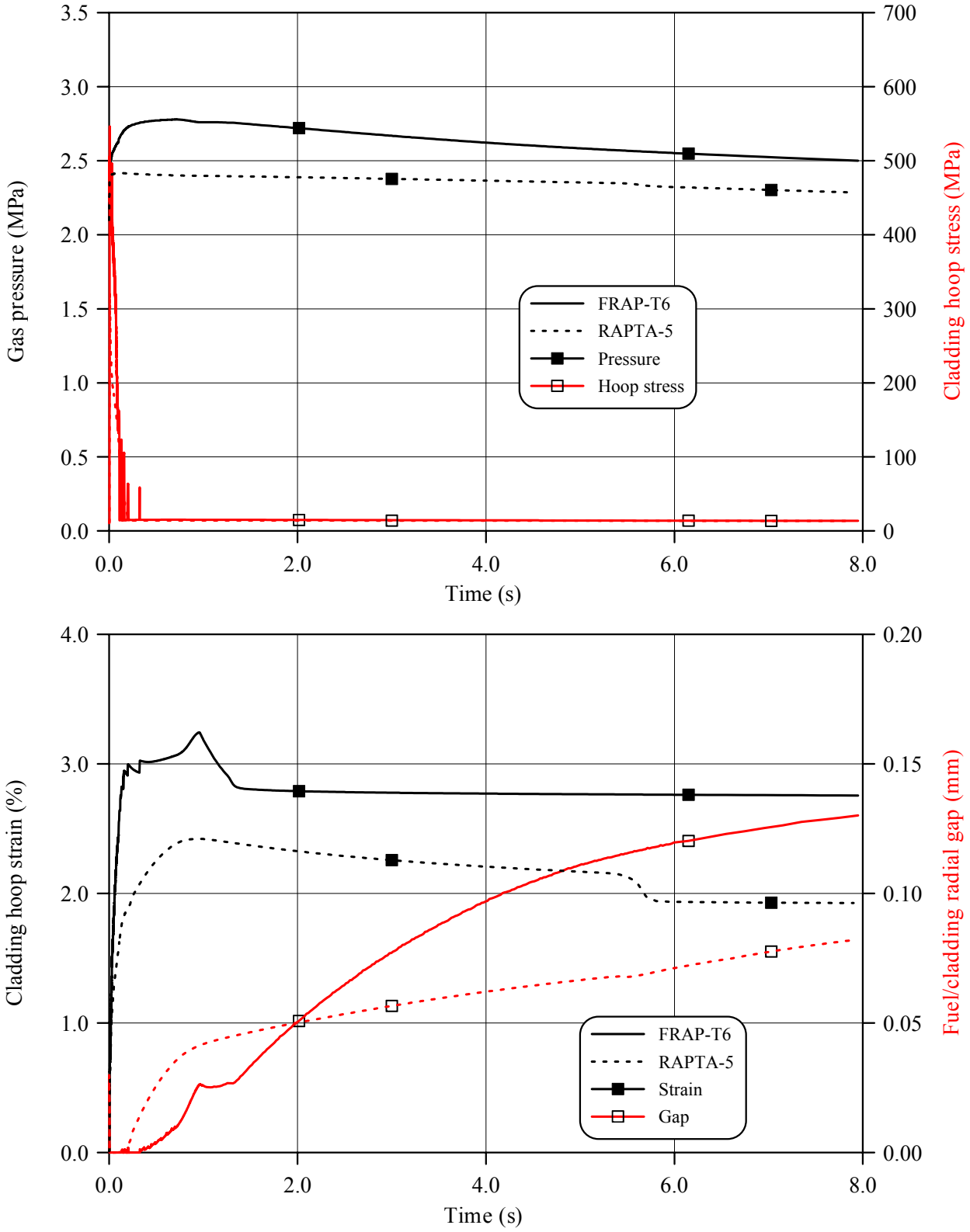


**Fig.E-1.7. Mechanical behavior of fuel rod # RT1 during the BIGR test in accordance with FRAP-T6/VVER and RAPTA-5 calculations**

# # RT1

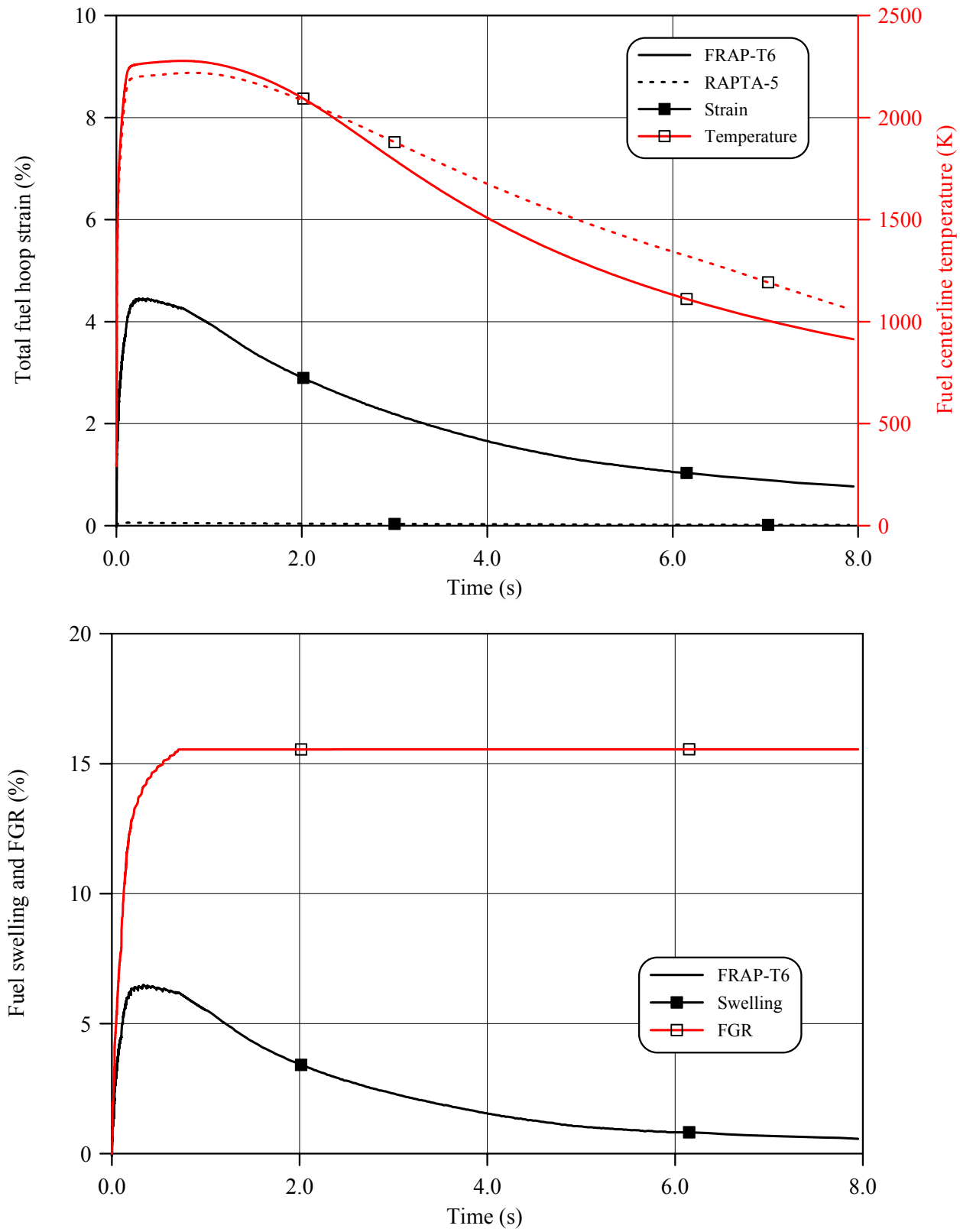


**Fig.E-1.8. Fuel behavior during the BIGR test of fuel rod # RT1 in accordance with FRAP-T6/VVER and RAPTA-5 calculations**

# # RT1

**Table E-1.3. Axial distribution of cladding average outer diameter in fuel rod # RT1***

| Axial coordinate (mm) | Cladding diameter (mm) | Axial coordinate (mm) | Cladding diameter (mm) | Axial coordinate (mm) | Cladding diameter (mm) | Axial coordinate (mm) | Cladding diameter (mm) |
|---|---|---|---|---|---|---|---|
| 30 | 9.200 | 68 | 9.238 | 106 | 9.248 | 144 | 9.336 |
| 32 | 9.197 | 70 | 9.250 | 108 | 9.265 | 146 | 9.293 |
| 34 | 9.213 | 72 | 9.252 | 110 | 9.248 | 148 | 9.228 |
| 36 | 9.226 | 74 | 9.263 | 112 | 9.220 | 150 | 9.237 |
| 38 | 9.239 | 76 | 9.264 | 114 | 9.198 | 152 | 9.294 |
| 40 | 9.235 | 78 | 9.249 | 116 | 9.245 | 154 | 9.354 |
| 42 | 9.214 | 80 | 9.257 | 118 | 9.304 | 156 | 9.360 |
| 44 | 9.203 | 82 | 9.266 | 120 | 9.344 | 158 | 9.303 |
| 46 | 9.220 | 84 | 9.283 | 122 | 9.308 | 160 | 9.246 |
| 48 | 9.227 | 86 | 9.310 | 124 | 9.244 | 162 | 9.277 |
| 50 | 9.235 | 88 | 9.321 | 126 | 9.221 | 164 | 9.349 |
| 52 | 9.226 | 90 | 9.309 | 128 | 9.268 | 166 | 9.426 |
| 54 | 9.184 | 92 | 9.315 | 130 | 9.310 | 168 | 9.338 |
| 56 | 9.160 | 94 | 9.321 | 132 | 9.325 | 170 | 9.181 |
| 58 | 9.168 | 96 | 9.352 | 134 | 9.312 | 172 | 9.097 |
| 60 | 9.185 | 98 | 9.358 | 136 | 9.289 | 174 | 9.065 |
| 62 | 9.211 | 100 | 9.299 | 138 | 9.306 | 176 | 9.075 |
| 64 | 9.236 | 102 | 9.219 | 140 | 9.340 | 178 | 9.073 |
| 66 | 9.235 | 104 | 9.217 | 142 | 9.346 | 180 | 9.315 |

* Measured value determined on the basis of profilometry data (16 azimuthal directions)

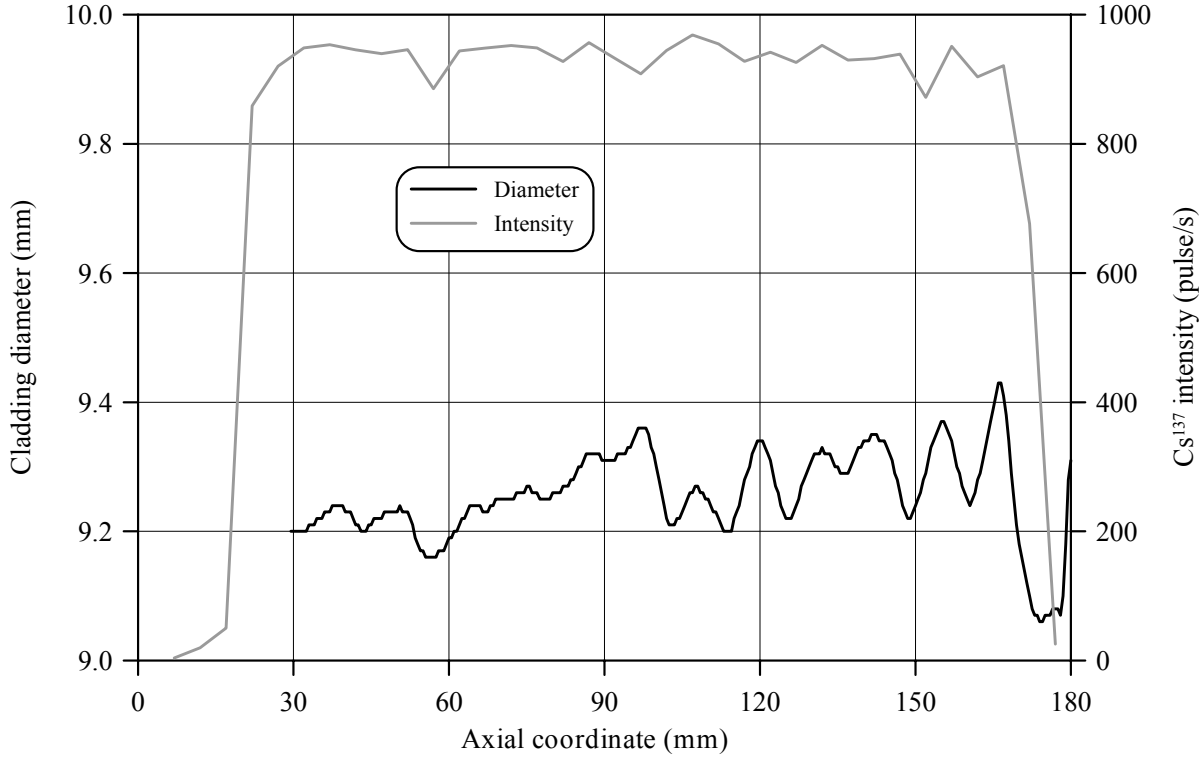


**Fig.E-1.9. Cladding measured average diameter and γ-scanning results for fuel rod # RT1**

**Table E-1.4. The PIE results for fuel rod # RT1**

| | Parameter | Value |
|---|---|---|
| 1. | Cladding outer diameter (mm): | |
| 1.1. | Maximum diameter of the bidimensional data sample in "fuel rod length - azimuthal angle" coordinates (mm) | 9.50 |
| 1.2. | Averaged azimuthal diameter and maximum diameter along the length selected from the sample of averaged azimuthal diameter (mm) | 9.43 |
| 1.3. | Averaged diameter of the bidimensional data sample in "fuel rod length - azimuthal angle" coordinates (mm) | 9.26 |
| 2. | Cladding maximum residual hoop strain (%) | 4.06 |
| 3. | Fuel pellet conditional diameter (mm) in cross-section*: | |
| | at 113 mm elevation | 7.64 |
| 4. | $ZrO_2$ outer thickness (μm) in cross-section: | |
| | at 113 mm elevation | 3–5 |
| 5. | $ZrO_2$ inner thickness (μm) in cross-section: | |
| | at 113 mm elevation | 0 |
| 6. | Parameters characterizing FGR: | |
| 6.1. | Gas composition (% by volume): | |
| | He | 86.08 |
| | $N_2$ | 0.70 |
| | $O_2$ | 0.13 |
| | Ar | 0.014 |
| | $CO_2$ | 0.011 |
| | Kr | 1.19 |
| | Xe | 11.88 |
| 6.2. | Free gas volume ($cm^3$) | 6.5 |
| 6.3. | Gas volume under normal conditions ($cm^3$) | 142.3 |
| 6.4. | Gas pressure under normal conditions (MPa) | 2.19 |
| 6.5. | FGR (%) | 22.8 |

* Reference value determined by the processing of fuel cross-section photographs

# # RT1

**Table E-1.5. Organized BIGR test results for fuel rod # RT1**

| Parameter | | Unit | Value | | |
|---|---|---|---|---|---|
| | | | Measured | Calculated | |
| | | | | FRAP-T6 | RAPTA-5 |
| 1. | Fuel burnup | MW d/kg U | 48.3 | 48.3 | 48.3 |
| 2. | Initial gas pressure | MPa | 2.1 | 2.1 | 2.1 |
| 3. | Energy deposition | cal/g fuel | 174.0 | 174.0 | 174.0 |
| 4. | Peak fuel enthalpy* | cal/g fuel | - | 142.9 | 141.6 |
| 5. | Fuel maximum temperature | K | - | 2313 | 2327 |
| 6. | Maximum temperature of cladding outer surface | K | - | 1111 | 1162 |
| 7. | Cladding burst | Failed, Unfailed | Unfailed | Unfailed | Unfailed |
| 8. | Cladding residual hoop strain** | % | 2.20 | 2.66 | 1.86 |
| 9. | Kr volume content in gas composition after the BIGR test | % | 1.19 | 1.67 | - |
| 10. | Xe volume content in gas composition after the BIGR test | % | 11.88 | 10.00 | - |

* Average value of peak fuel enthalpy is 142.2 cal/g fuel

** Average value along the fuel stack length

# *Appendix E–2*

# *Individual Characteristics of Fuel Rod # RT2 after the BIGR Test*

# # RT2

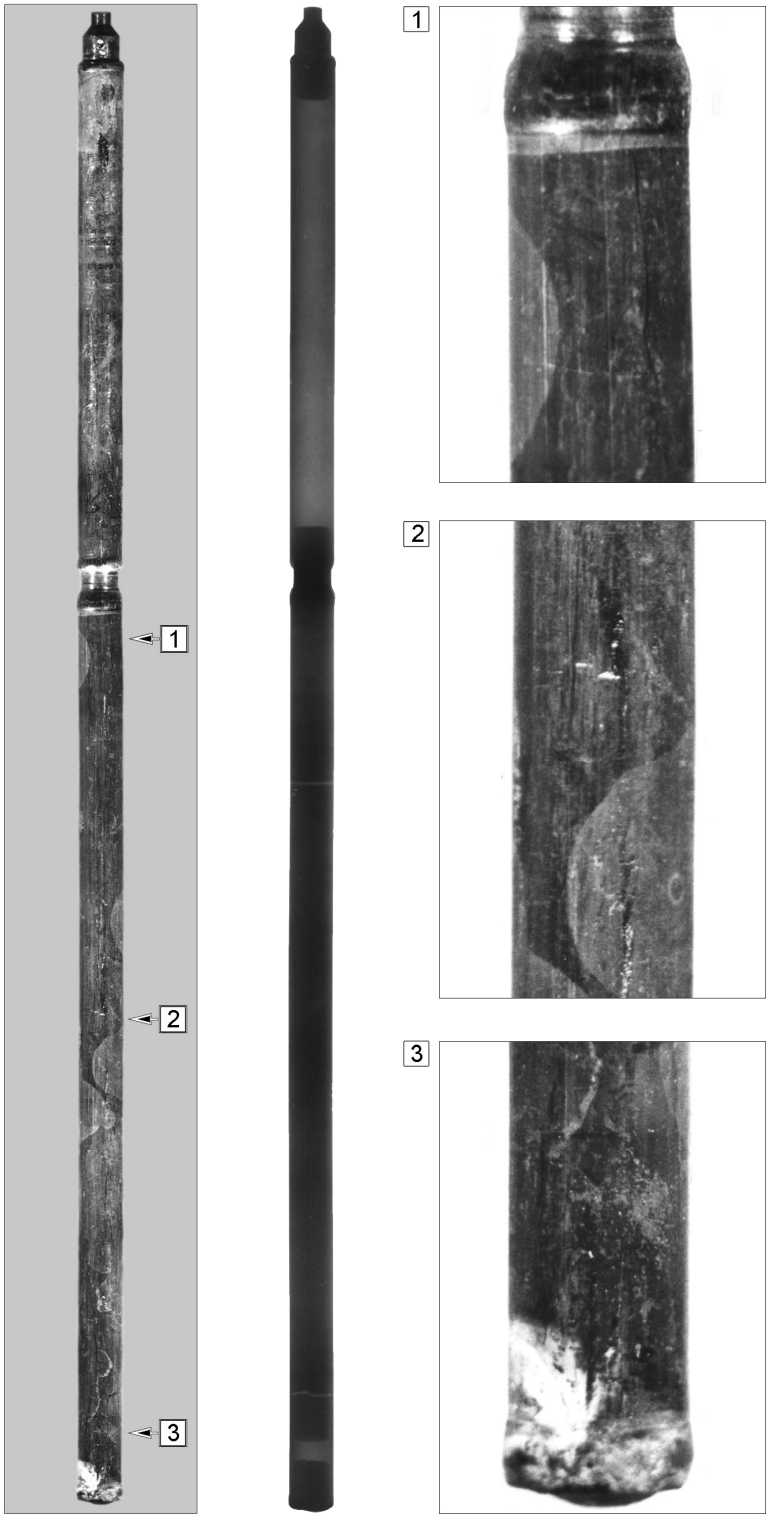


**Fig.E-2.1. Appearance of unfailed fuel rod # RT2 after the BIGR test (photographs and X-ray photograph)**

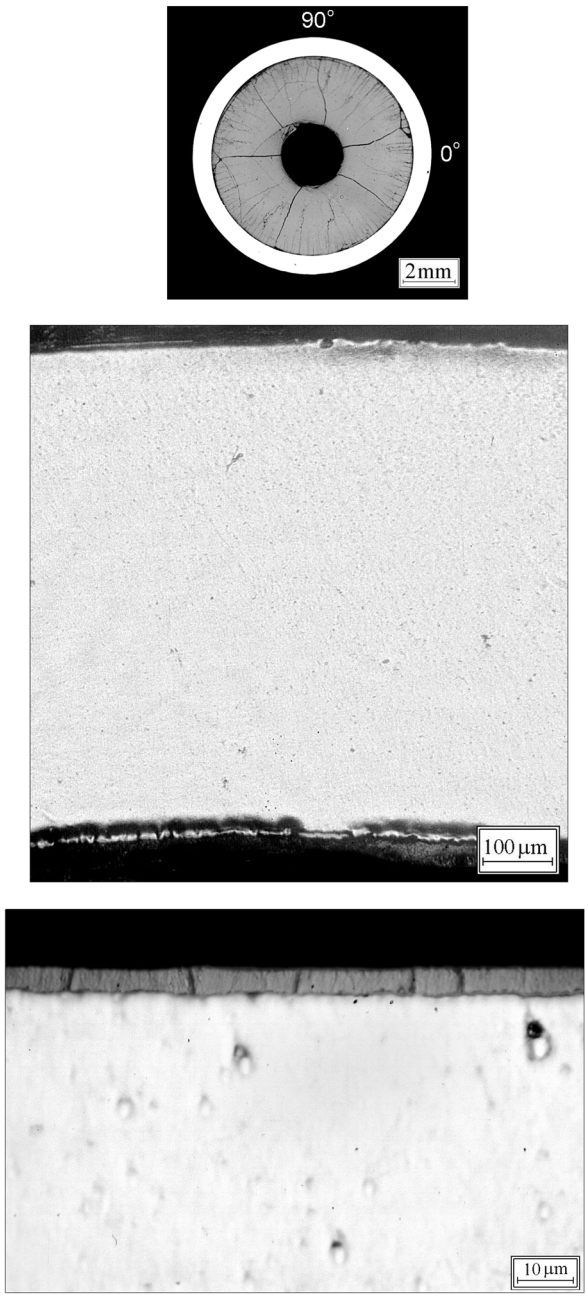


**Fig.E-2.2. Cross-section and cladding microstructure of fuel rod # RT2 at 99 mm elevation (from low cap)**

# # RT2

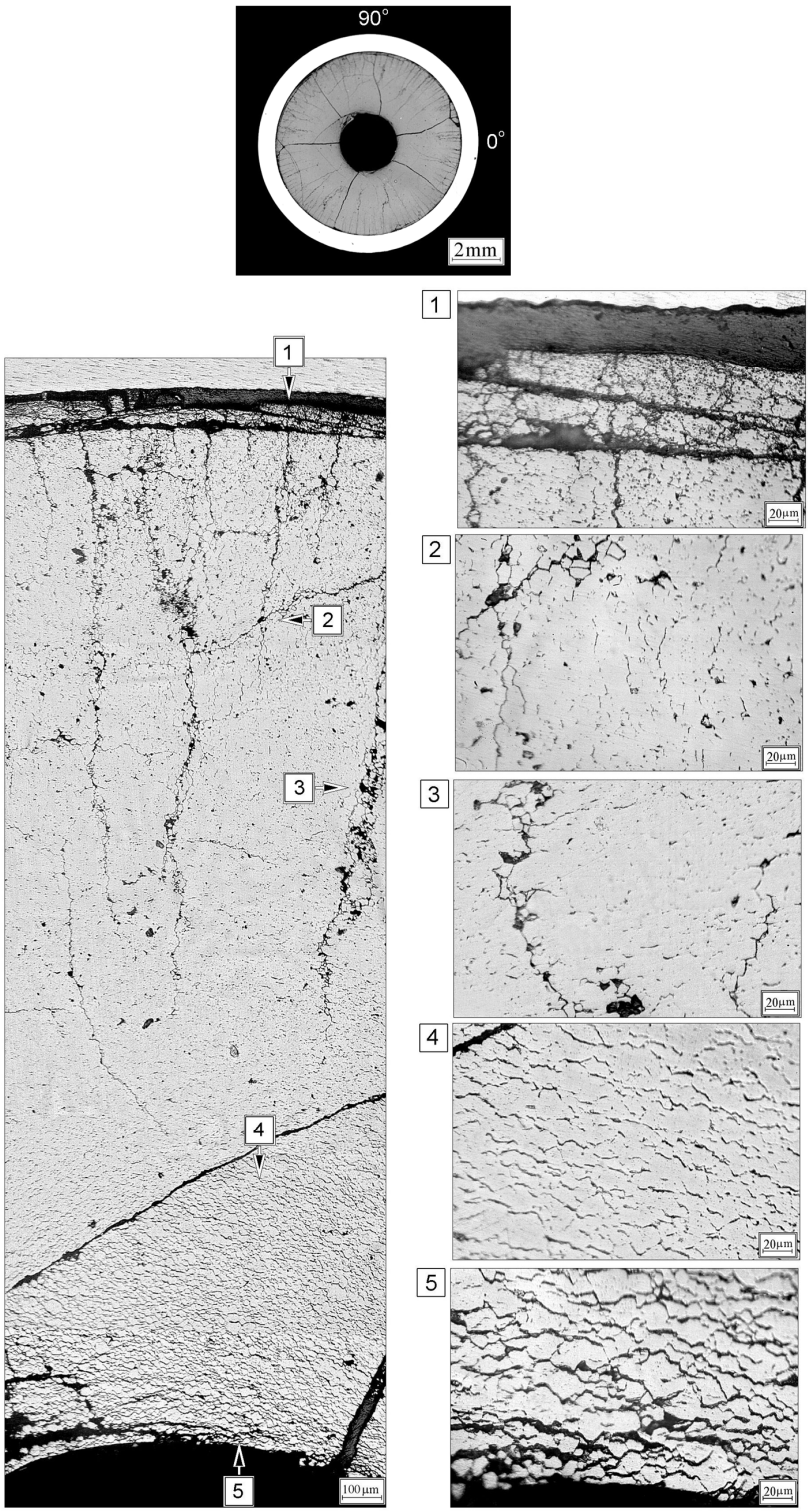


**Fig.E-2.3. Cross-section and fuel microstructure of fuel rod # RT2 at 99 mm elevation (from low cap)**

**Table E-2.1. Time dependent energy characteristics of fuel rod # RT2**

| Time (s) | Relative reactor power (current/ maximum value) (per-unit) | Cumulative number of fissions in fuel rod (fiss) x$10^{-14}$ | Power of fuel rod[1)2)] (kW) | Energy deposition | | Fuel enthalpy[3)] | |
|---|---|---|---|---|---|---|---|
| | | | | (cal/g fuel) | (J/g fuel) | FRAP-T6 | RAPTA-5 |
| 0.000 | 7.10E-02 | 0.000 | 0.000 | 0.000 | 0.000 | 0.000 | 0.000 |
| 0.001 | 4.44E-01 | 0.516 | 2415 | 5.397 | 22.59 | 5.829 | 5.110 |
| 0.002 | 9.04E-01 | 1.777 | 4917 | 18.76 | 78.52 | 19.119 | 18.520 |
| 0.003 | 9.40E-01 | 3.576 | 5115 | 37.83 | 158.4 | 37.673 | 37.576 |
| 0.004 | 6.20E-01 | 5.042 | 3374 | 53.34 | 223.3 | 52.772 | 52.916 |
| 0.005 | 3.08E-01 | 5.890 | 1673 | 62.41 | 261.3 | 61.506 | 61.691 |
| 0.006 | 1.56E-01 | 6.302 | 846.7 | 66.68 | 279.2 | 65.486 | 65.655 |
| 0.007 | 9.88E-02 | 6.530 | 537.4 | 69.11 | 289.3 | 67.641 | 67.796 |
| 0.008 | 7.42E-02 | 6.685 | 403.6 | 70.79 | 296.4 | 69.046 | 69.202 |
| 0.009 | 6.61E-02 | 6.812 | 359.4 | 72.14 | 302.0 | 70.151 | 70.318 |
| 0.010 | 6.38E-02 | 6.938 | 347.0 | 73.41 | 307.3 | 71.177 | 71.364 |
| 0.012 | 6.59E-02 | 7.176 | 358.7 | 75.94 | 317.9 | 73.233 | 73.405 |
| 0.014 | 6.95E-02 | 7.431 | 378.0 | 78.64 | 329.3 | 75.489 | 75.808 |
| 0.016 | 6.71E-02 | 7.688 | 365.4 | 81.37 | 340.6 | 77.764 | 78.147 |
| 0.018 | 6.08E-02 | 7.926 | 330.8 | 83.91 | 351.3 | 79.884 | 80.304 |
| 0.020 | 5.21E-02 | 8.138 | 283.6 | 86.14 | 360.6 | 81.698 | 82.379 |
| 0.022 | 4.33E-02 | 8.309 | 235.8 | 88.02 | 368.5 | 83.194 | 83.861 |
| 0.024 | 3.65E-02 | 8.460 | 198.7 | 89.58 | 375.0 | 84.396 | 85.038 |
| 0.026 | 3.20E-02 | 8.590 | 174.5 | 90.92 | 380.7 | 85.397 | 86.178 |
| 0.028 | 2.96E-02 | 8.699 | 161.1 | 92.13 | 385.7 | 86.280 | 87.089 |
| 0.030 | 2.88E-02 | 8.809 | 156.8 | 93.27 | 390.5 | 87.109 | 87.794 |
| 0.050 | 2.90E-02 | 9.936 | 157.8 | 105.2 | 440.4 | 95.999 | 97.218 |
| 0.070 | 2.33E-02 | 10.90 | 126.9 | 115.4 | 483.3 | 103.409 | 104.960 |
| 0.090 | 1.92E-02 | 11.70 | 104.8 | 123.8 | 518.4 | 109.210 | 111.040 |
| 0.110 | 1.06E-02 | 12.27 | 57.66 | 129.9 | 544.0 | 113.001 | 115.210 |
| 0.130 | 3.90E-03 | 12.51 | 21.44 | 132.6 | 555.1 | 114.296 | 116.180 |
| 0.150 | 1.49E-03 | 12.61 | 8.302 | 133.6 | 559.2 | 114.072 | 115.740 |
| 0.200 | 4.00E-04 | 12.68 | 2.414 | 134.4 | 562.6 | 112.792 | 113.770 |
| 1.000 | 3.59E-05 | 12.79 | 0.300 | 135.9 | 568.8 | 96.970 | 96.035 |
| 10.00 | 4.15E-06 | 12.98 | 0.044 | 139.3 | 583.1 | 20.562 | 17.632 |
| 100.0 | 8.08E-08 | 13.07 | 0.007 | 141.8 | 593.8 | 4.773 | 4.276 |
| 1000 | 3.16E-13 | 13.08 | 1.59E-04 | 143.0 | 598.8 | 0.000 | 0.000 |

1) Average values determined in accordance with results of RRC KI and VNIIEF calculations

2) Maximum power value is 5440.5 kW (t=0.0026 s)

3) Average radial value

# # RT2

**Table E-2.2. Radial energy characteristics of fuel rod # RT2***

| Parameters | Coordinates of fuel radial layers (mm) | | | |
|---|---|---|---|---|
| | 1 layer (1.23-2.82) | 2 layer (2.82-3.44) | 3 layer (3.44-3.71) | 4 layer (3.71-3.795) |
| Number of fissions $x10^{-14}$ (fiss) | 5.879 | 3.819 | 2.269 | 1.103 |
| Fission density $x10^{-13}$ (fiss/g fuel) | 1.878 | 2.008 | 2.444 | 3.629 |
| Power** (kW) | 2426 | 1585 | 955.5 | 474.6 |
| Energy deposition (cal/g fuel) | 128.6 | 137.3 | 167.4 | 252.3 |
| Energy deposition (J/g fuel) | 538.6 | 574.9 | 700.8 | 1056 |
| Energy deposition*** (per-unit) | 0.510 | 0.544 | 0.663 | 1.000 |

* Average values were determined in accordance with results of RRC KI and VNIIEF calculations

** The power for the entire length of each layer at time 0.0026 s

*** Energy deposition in current layer/energy deposition in $4^{th}$ layer

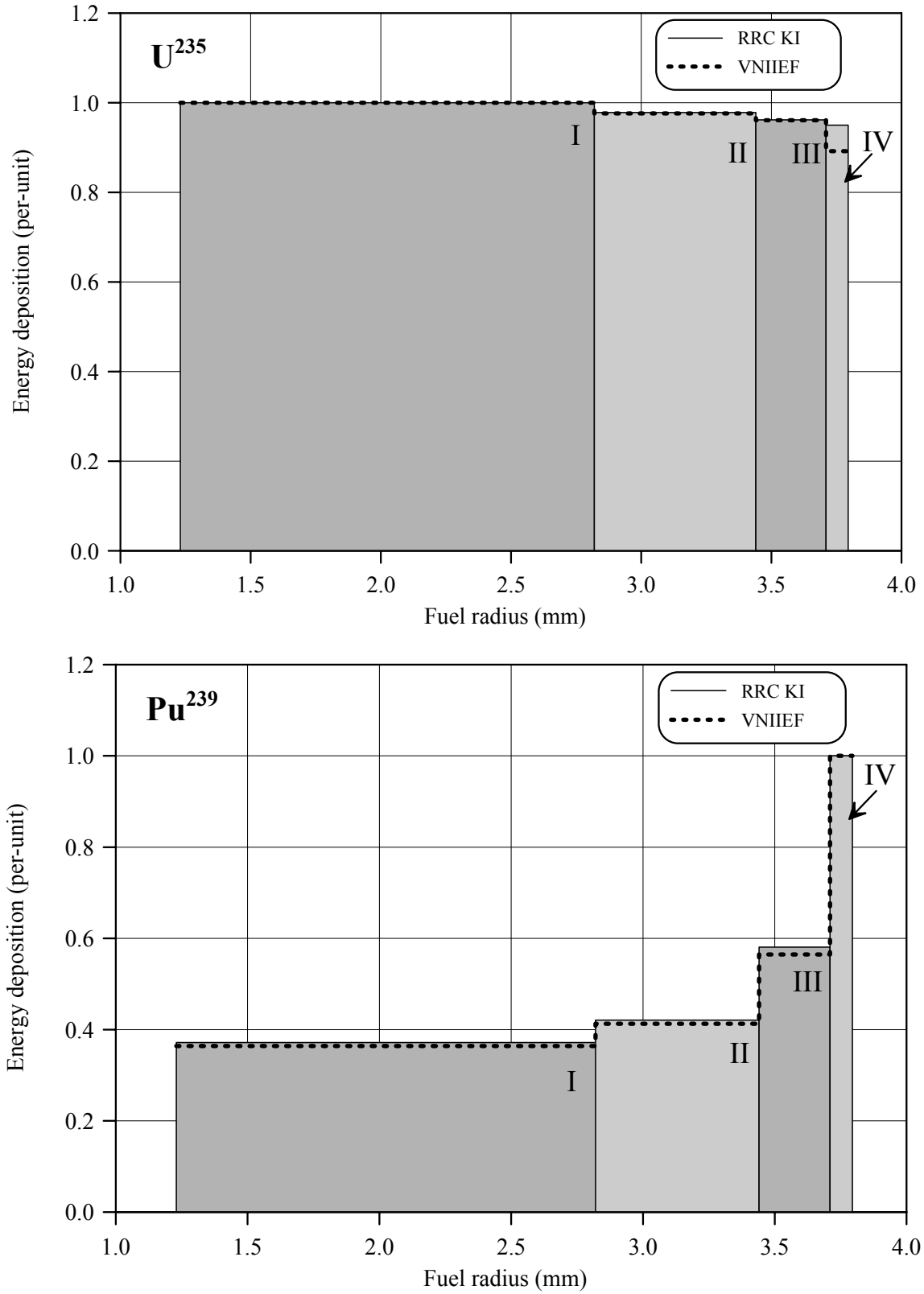


**Fig.E-2.4. $U^{235}$ and $Pu^{239}$ radial distribution of energy deposition for fuel rod # RT2**

# # RT2

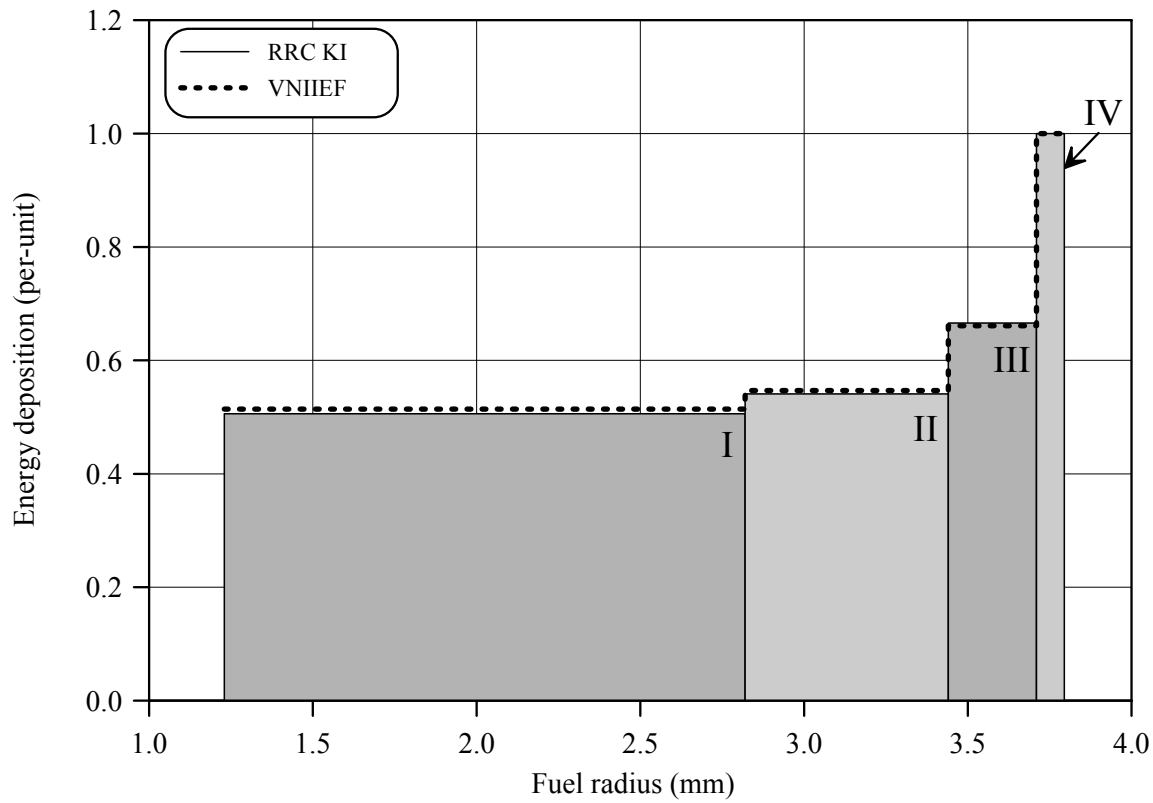


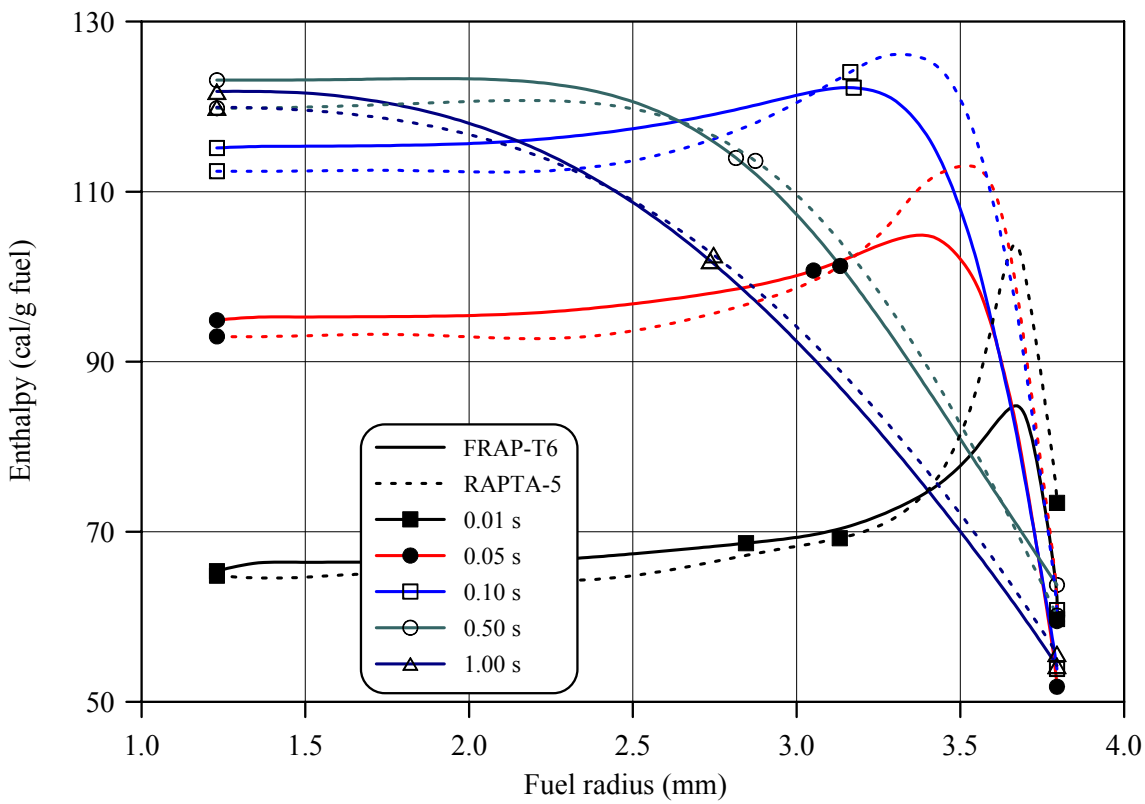


**Fig.E-2.5. Radial distribution of energy deposition and fuel enthalpy for fuel rod # RT2**

# # RT2

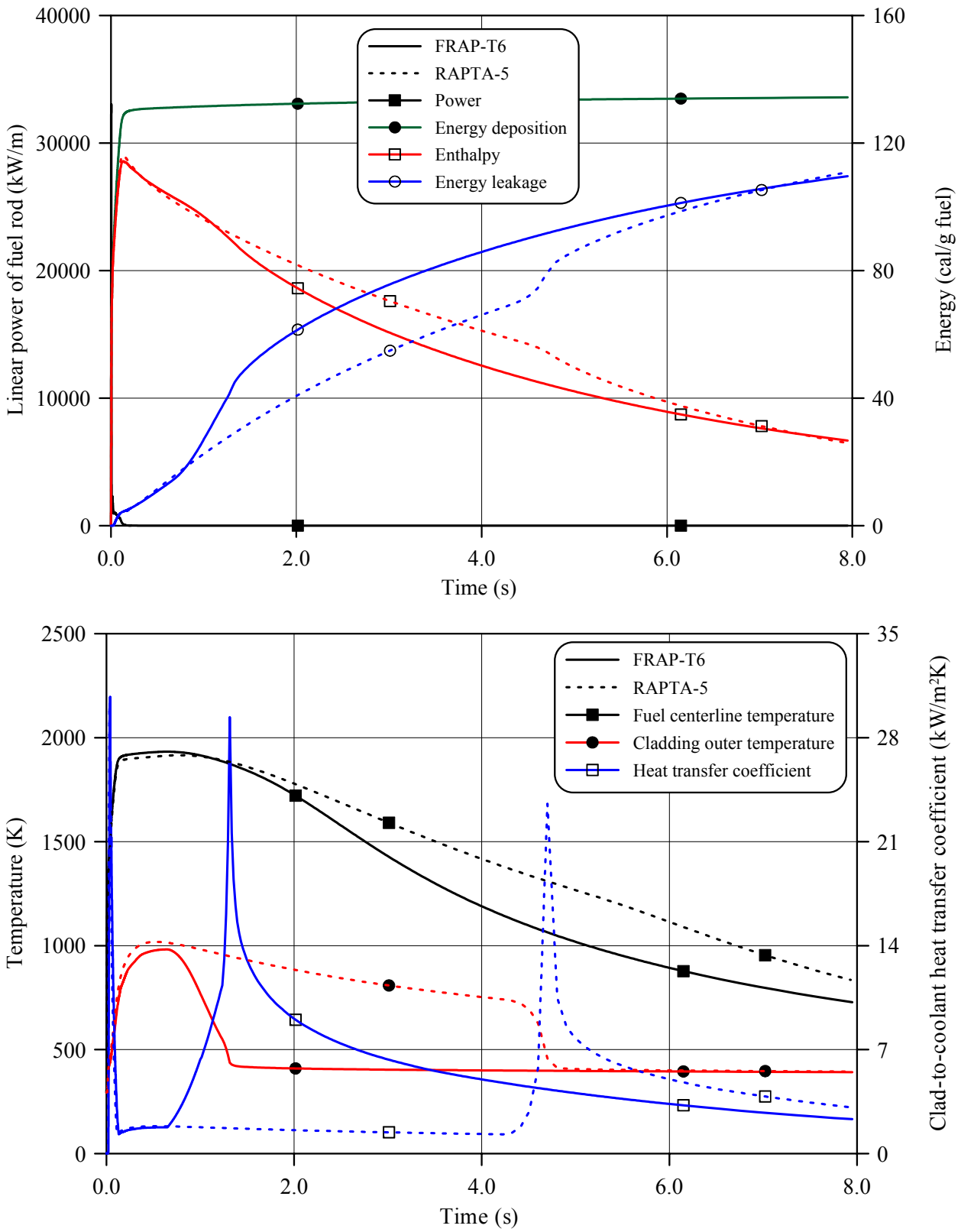


**Fig.E-2.6. Thermal history of fuel rod # RT2 during the BIGR test in accordance with FRAP-T6/VVER and RAPTA-5 calculations**

# # RT2

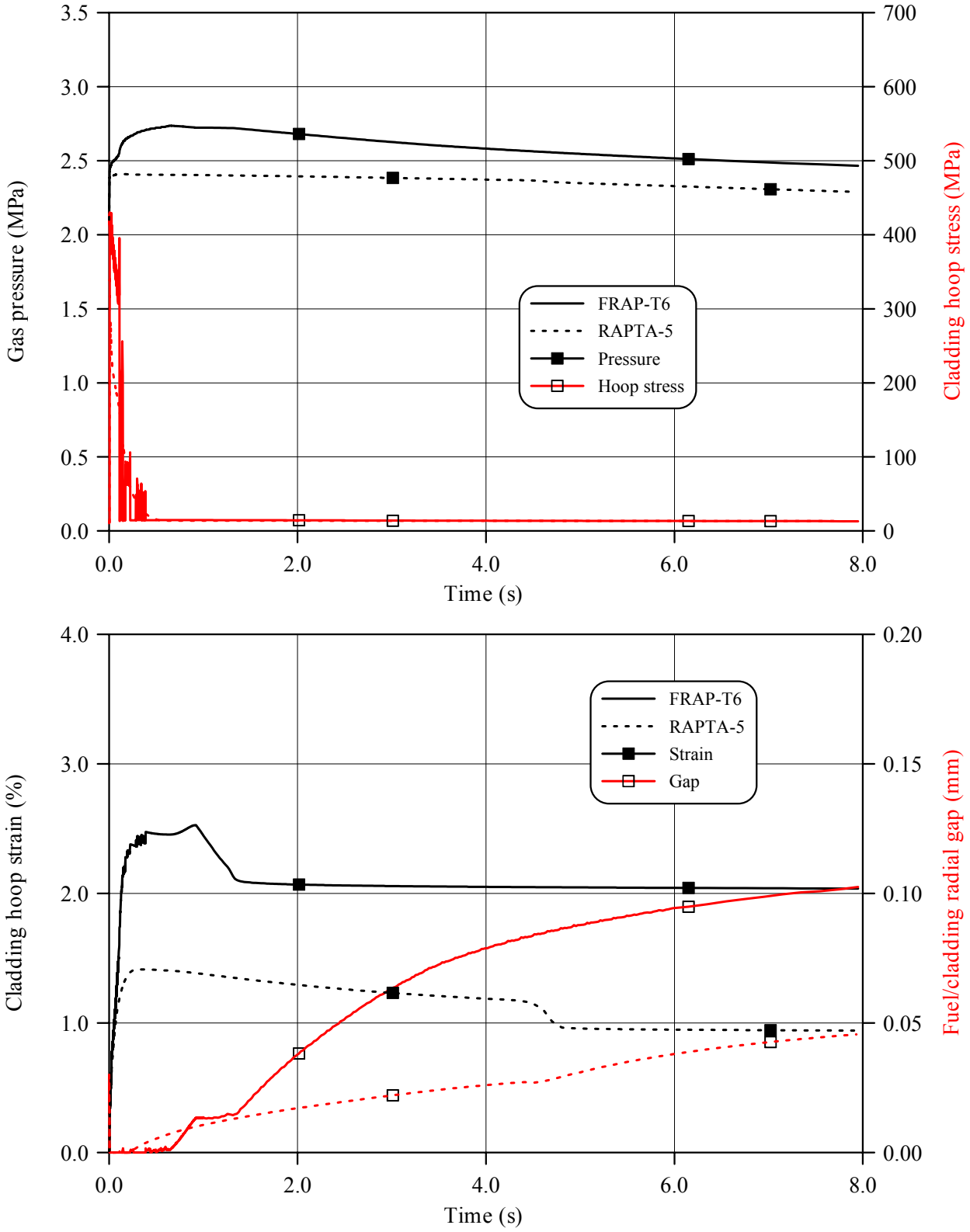


**Fig.E-2.7. Mechanical behavior of fuel rod # RT2 during the BIGR test in accordance with FRAP-T6/VVER and RAPTA-5 calculations**

# # RT2

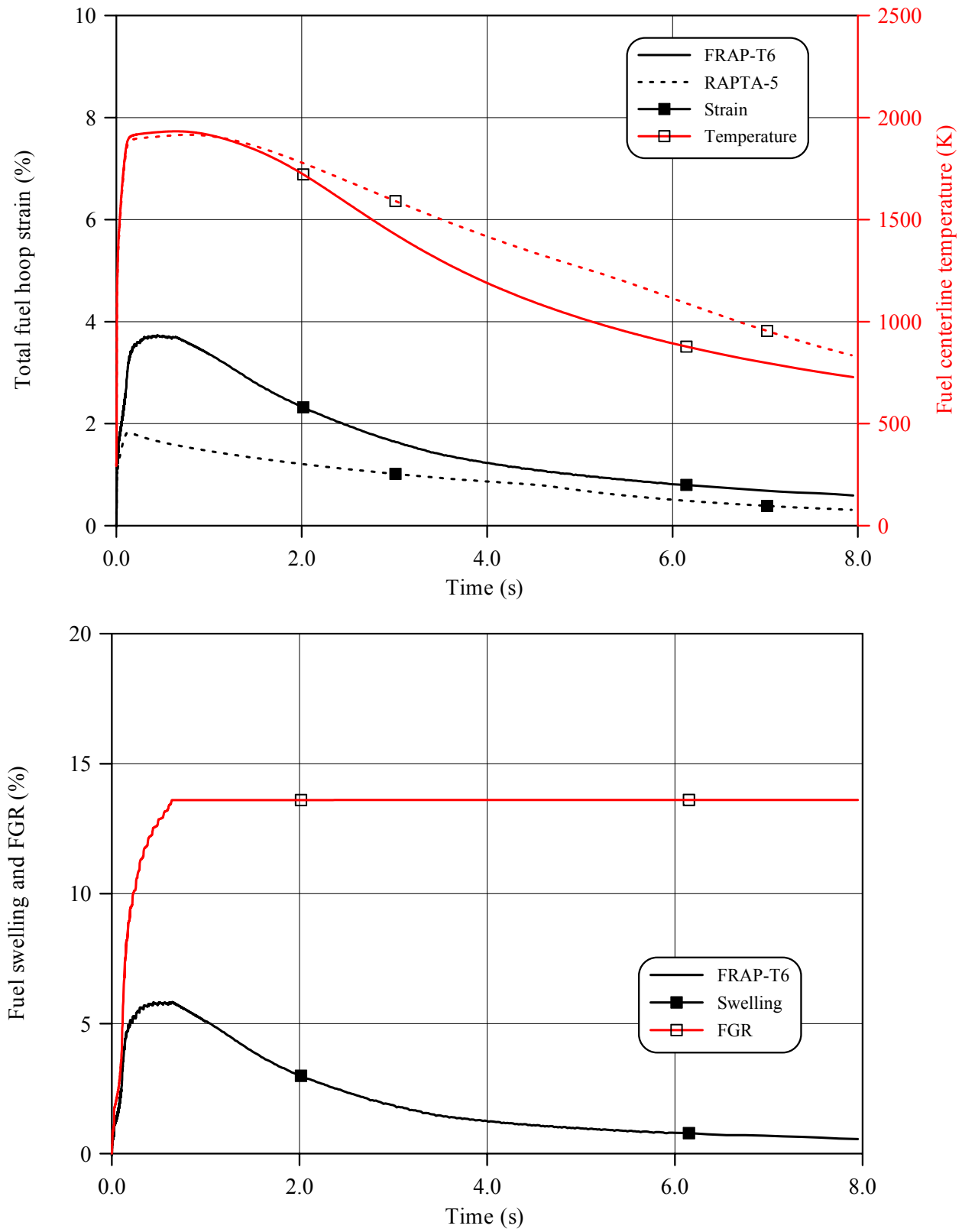


**Fig.E-2.8. Fuel behavior during the BIGR test of fuel rod # RT2 in accordance with FRAP-T6/VVER and RAPTA-5 calculations**

# # RT2

**Table E-2.3. Axial distribution of cladding average outer diameter in fuel rod # RT2***

| Axial coordinate (mm) | Cladding diameter (mm) | Axial coordinate (mm) | Cladding diameter (mm) | Axial coordinate (mm) | Cladding diameter (mm) | Axial coordinate (mm) | Cladding diameter (mm) |
|---|---|---|---|---|---|---|---|
| 30 | 9.102 | 68 | 9.112 | 106 | 9.116 | 144 | 9.124 |
| 32 | 9.103 | 70 | 9.114 | 108 | 9.123 | 146 | 9.129 |
| 34 | 9.105 | 72 | 9.112 | 110 | 9.125 | 148 | 9.130 |
| 36 | 9.108 | 74 | 9.114 | 112 | 9.128 | 150 | 9.128 |
| 38 | 9.098 | 76 | 9.111 | 114 | 9.129 | 152 | 9.133 |
| 40 | 9.112 | 78 | 9.112 | 116 | 9.129 | 154 | 9.134 |
| 42 | 9.111 | 80 | 9.116 | 118 | 9.118 | 156 | 9.134 |
| 44 | 9.110 | 82 | 9.119 | 120 | 9.132 | 158 | 9.135 |
| 46 | 9.113 | 84 | 9.111 | 122 | 9.137 | 160 | 9.128 |
| 48 | 9.108 | 86 | 9.126 | 124 | 9.140 | 162 | 9.119 |
| 50 | 9.108 | 88 | 9.125 | 126 | 9.137 | 164 | 9.112 |
| 52 | 9.109 | 90 | 9.124 | 128 | 9.136 | 166 | 9.098 |
| 54 | 9.108 | 92 | 9.127 | 130 | 9.129 | 168 | 9.072 |
| 56 | 9.112 | 94 | 9.126 | 132 | 9.135 | 170 | 9.067 |
| 58 | 9.120 | 96 | 9.121 | 134 | 9.139 | 172 | 9.065 |
| 60 | 9.118 | 98 | 9.124 | 136 | 9.138 | 174 | 9.042 |
| 62 | 9.111 | 100 | 9.127 | 138 | 9.132 | 176 | 9.141 |
| 64 | 9.119 | 102 | 9.129 | 140 | 9.131 | 178 | 9.433 |
| 66 | 9.120 | 104 | 9.127 | 142 | 9.124 | 180 | 8.937 |

* Measured value determined on the basis of profilometry data (16 azimuthal directions)

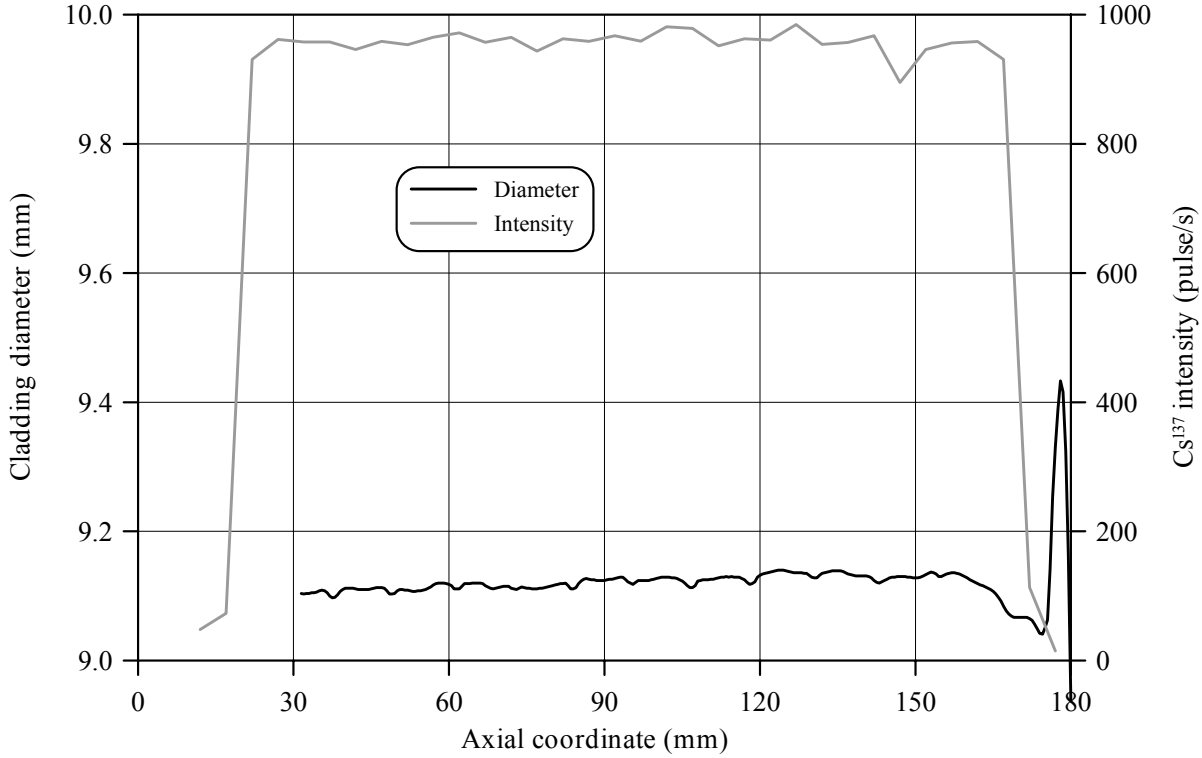


**Fig.E-2.9. Cladding measured average diameter and γ-scanning results for fuel rod # RT2**

**Table E-2.4. The PIE results for fuel rod # RT2**

| | Parameter | Value |
|---|---|---|
| 1. | Cladding outer diameter (mm): | |
| 1.1. | Maximum diameter of the bidimensional data sample in "fuel rod length - azimuthal angle" coordinates (mm) | 9.15 |
| 1.2. | Averaged azimuthal diameter and maximum diameter along the length selected from the sample of averaged azimuthal diameter (mm) | 9.14 |
| 1.3. | Averaged diameter of the bidimensional data sample in "fuel rod length - azimuthal angle" coordinates (mm) | 9.12 |
| 2. | Cladding maximum residual hoop strain (%) | 0.85 |
| 3. | Fuel pellet conditional diameter (mm) in cross-section*: | |
| | at 99 mm elevation | 7.64 |
| 4. | $ZrO_2$ outer thickness (μm) in cross-section: | |
| | at 99 mm elevation | 3-5 |
| 5. | $ZrO_2$ inner thickness (μm) in cross-section: | |
| | at 99 mm elevation | 0 |
| 6. | Parameters characterizing FGR: | |
| 6.1. | Gas composition (% by volume): | |
| | He | 86.08 |
| | $N_2$ | 4.05 |
| | $O_2$ | 0.12 |
| | Ar | 0.018 |
| | $CO_2$ | 0.010 |
| | Kr | 0.90 |
| | Xe | 8.97 |
| 6.2. | Free gas volume ($cm^3$) | 6.2 |
| 6.3. | Gas volume under normal conditions ($cm^3$) | 137.5 |
| 6.4. | Gas pressure under normal conditions (MPa) | 2.22 |
| 6.5. | FGR (%) | 16.1 |

* Reference value determined by the processing of fuel cross-section photographs

# # RT2

**Table E-2.5. Organized BIGR test results for fuel rod # RT2**

| Parameter | | Unit | Value | | |
|---|---|---|---|---|---|
| | | | Measured | Calculated | |
| | | | | FRAP-T6 | RAPTA-5 |
| 1. | Fuel burnup | MW d/kg U | 48.0 | 48.0 | 48.0 |
| 2. | Initial gas pressure | MPa | 2.1 | 2.1 | 2.1 |
| 3. | Energy deposition | cal/g fuel | 143.0 | 143.0 | 143.0 |
| 4. | Peak fuel enthalpy* | cal/g fuel | - | 114.3 | 116.2 |
| 5. | Fuel maximum temperature | K | - | 1963 | 2011 |
| 6. | Maximum temperature of cladding outer surface | K | - | 982 | 1019 |
| 7. | Cladding burst | Failed, Unfailed | Unfailed | Unfailed | Unfailed |
| 8. | Cladding residual hoop strain** | % | 0.63 | 1.94 | 0.88 |
| 9. | Kr volume content in gas composition after the BIGR test | % | 0.90 | 1.50 | - |
| 10. | Xe volume content in gas composition after the BIGR test | % | 8.97 | 9.01 | - |

* Average value of peak fuel enthalpy is 115.2 cal/g fuel

** Average value along the fuel stack length

# *Appendix E–3*

# *Individual Characteristics of Fuel Rod # RT3 after the BIGR Test*

# # RT3

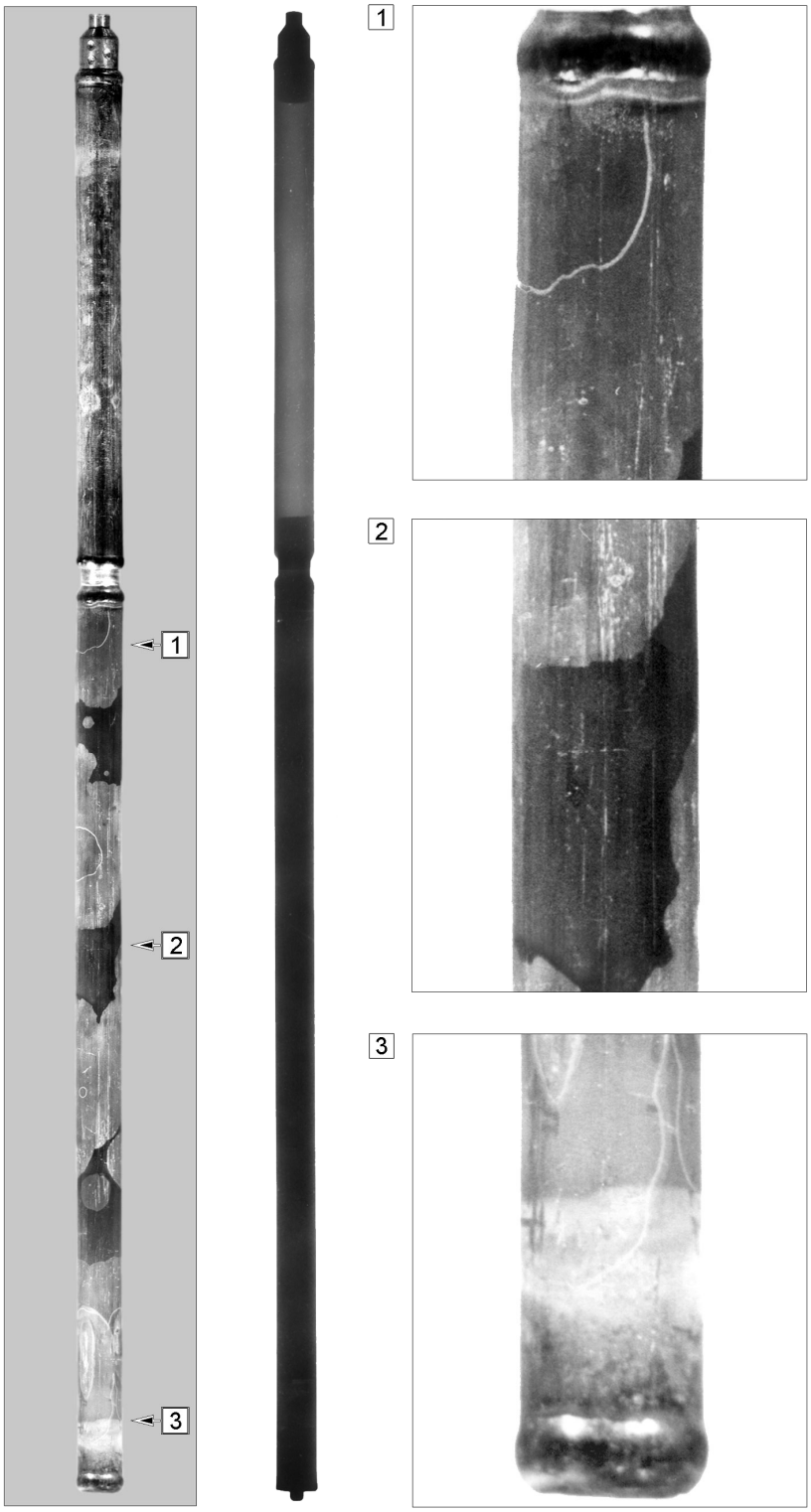


**Fig.E-3.1. Appearance of unfailed fuel rod # RT3 after the BIGR test (photographs and X-ray photograph)**

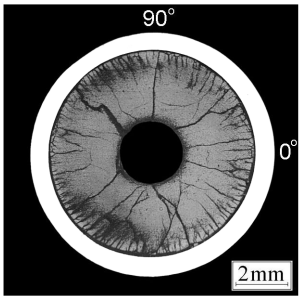


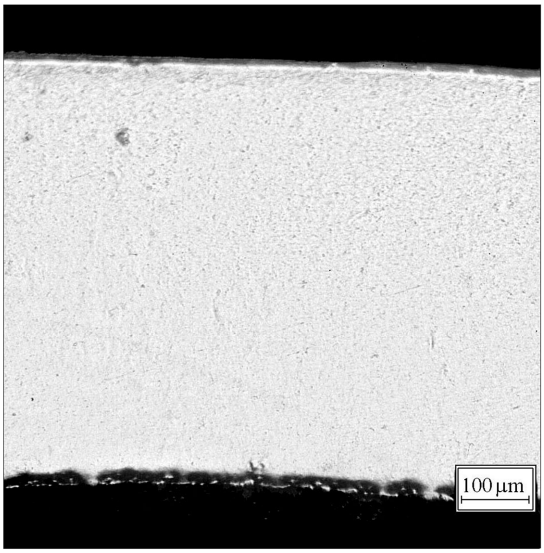


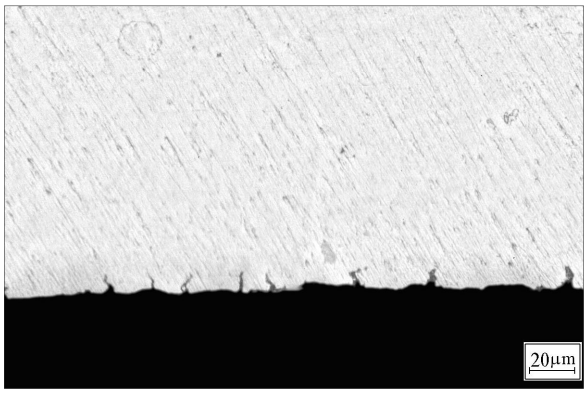


**Fig.E-3.2. Cross-section and cladding microstructure of fuel rod # RT3 at 113 mm elevation (from low cap)**

# # RT3

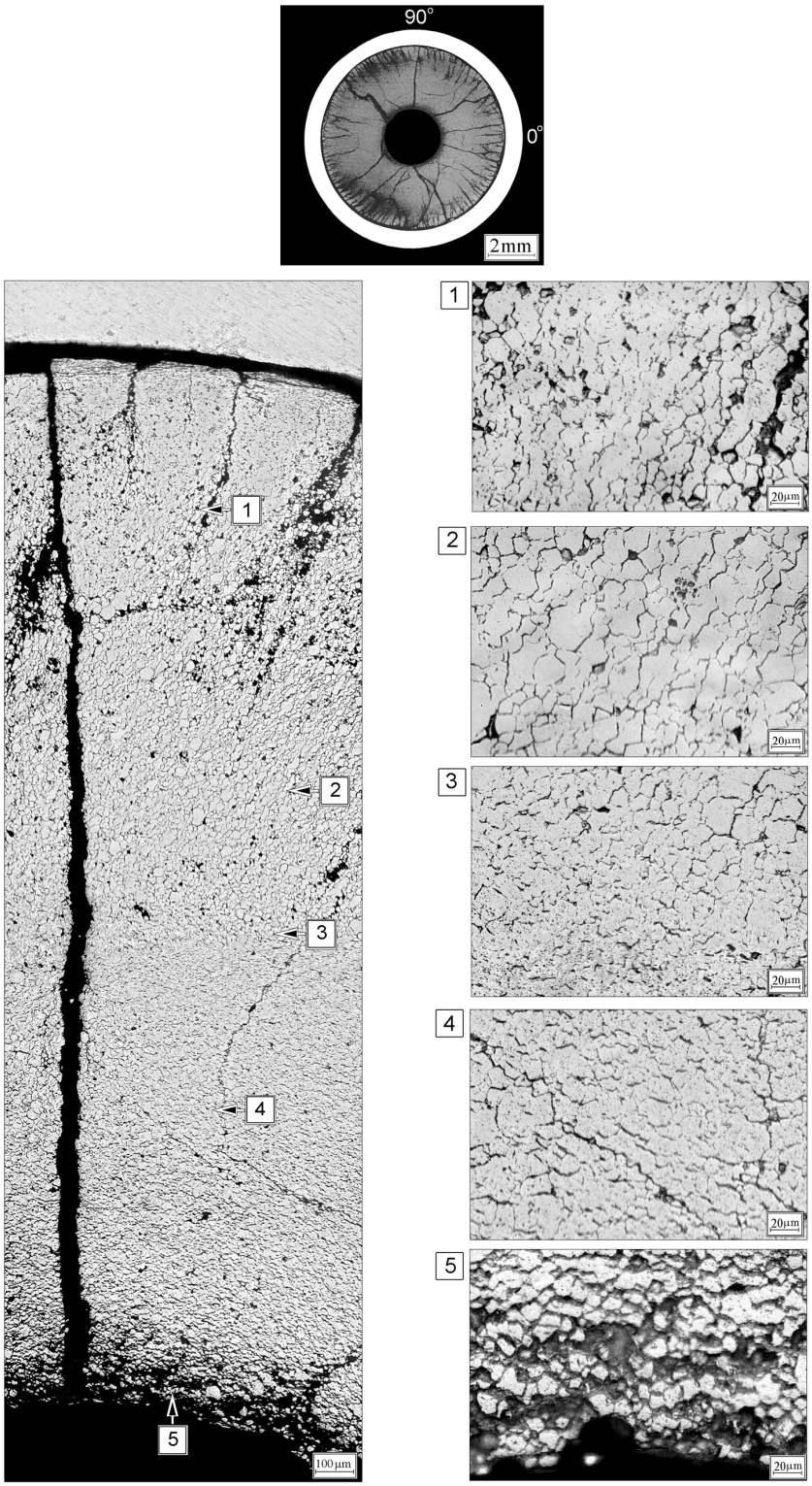


**Fig.E-3.3. Cross-section and fuel microstructure of fuel rod # RT3 at 113 mm elevation (from low cap)**

**Table E-3.1. Time dependent energy characteristics of fuel rod # RT3**

| Time (s) | Relative reactor power (current/ maximum value) (per-unit) | Cumulative number of fissions in fuel rod (fiss) x$10^{-14}$ | Power of fuel rod[1)2)] (kW) | Energy deposition | | Fuel enthalpy[3)] | |
|---|---|---|---|---|---|---|---|
| | | | | (cal/g fuel) | (J/g fuel) | FRAP-T6 | RAPTA-5 |
| 0.000 | 2.09E-02 | 0.000 | 0.000 | 0.000 | 0.000 | 0.000 | 0.000 |
| 0.001 | 1.97E-01 | 0.080 | 408.2 | 2.791 | 11.68 | 3.323 | 2.662 |
| 0.002 | 6.18E-01 | 0.376 | 1283 | 13.35 | 55.89 | 14.463 | 13.272 |
| 0.003 | 1.00E+00 | 1.028 | 2076 | 36.58 | 153.1 | 37.846 | 36.544 |
| 0.004 | 6.81E-01 | 1.702 | 1413 | 60.68 | 254.1 | 61.942 | 60.481 |
| 0.005 | 2.93E-01 | 2.065 | 608.2 | 73.47 | 307.6 | 74.603 | 72.889 |
| 0.006 | 1.48E-01 | 2.228 | 307.8 | 79.25 | 331.8 | 80.187 | 78.245 |
| 0.007 | 8.06E-02 | 2.310 | 167.3 | 82.23 | 344.3 | 82.916 | 80.850 |
| 0.008 | 5.58E-02 | 2.361 | 115.7 | 84.04 | 351.8 | 84.446 | 82.319 |
| 0.009 | 4.91E-02 | 2.401 | 102.0 | 85.45 | 357.7 | 85.585 | 83.429 |
| 0.010 | 4.78E-02 | 2.440 | 99.15 | 86.76 | 363.2 | 86.639 | 84.475 |
| 0.012 | 5.33E-02 | 2.514 | 110.7 | 89.50 | 374.7 | 88.872 | 86.778 |
| 0.014 | 6.59E-02 | 2.606 | 136.7 | 92.76 | 388.4 | 91.647 | 89.527 |
| 0.016 | 7.19E-02 | 2.715 | 149.2 | 96.53 | 404.1 | 94.924 | 92.891 |
| 0.018 | 6.92E-02 | 2.820 | 143.6 | 100.4 | 420.4 | 98.329 | 96.463 |
| 0.020 | 5.73E-02 | 2.915 | 119.0 | 103.9 | 434.9 | 101.320 | 99.371 |
| 0.022 | 4.57E-02 | 2.995 | 94.94 | 106.7 | 446.7 | 103.683 | 101.860 |
| 0.024 | 3.61E-02 | 3.062 | 74.92 | 108.9 | 456.1 | 105.485 | 103.670 |
| 0.026 | 2.90E-02 | 3.112 | 60.31 | 110.7 | 463.5 | 106.859 | 105.120 |
| 0.028 | 2.43E-02 | 3.148 | 50.46 | 112.1 | 469.4 | 107.931 | 106.030 |
| 0.030 | 2.29E-02 | 3.186 | 47.61 | 113.4 | 474.7 | 108.843 | 106.940 |
| 0.050 | 2.33E-02 | 3.558 | 48.44 | 126.5 | 529.7 | 118.563 | 116.950 |
| 0.070 | 1.88E-02 | 3.877 | 39.07 | 138.0 | 577.8 | 126.855 | 125.630 |
| 0.090 | 1.47E-02 | 4.139 | 30.65 | 147.2 | 616.4 | 133.304 | 132.350 |
| 0.110 | 7.95E-03 | 4.313 | 16.57 | 153.5 | 642.7 | 137.205 | 136.340 |
| 0.130 | 2.98E-03 | 4.394 | 6.240 | 156.3 | 654.5 | 138.624 | 137.210 |
| 0.150 | 1.13E-03 | 4.418 | 2.415 | 157.3 | 658.8 | 138.338 | 136.620 |
| 0.200 | 3.05E-04 | 4.440 | 0.701 | 158.2 | 662.4 | 136.674 | 134.300 |
| 1.000 | 2.77E-05 | 4.477 | 0.089 | 159.8 | 669.2 | 116.316 | 113.690 |
| 10.00 | 3.16E-06 | 4.537 | 0.013 | 163.6 | 685.1 | 23.629 | 24.851 |
| 100.0 | 6.15E-08 | 4.567 | 0.002 | 166.5 | 696.9 | 4.865 | 4.419 |
| 1000 | 2.40E-13 | 4.568 | 4.46E-05 | 167.9 | 702.8 | 0.000 | 0.000 |

1) Average values determined in accordance with results of RRC KI and VNIIEF calculations

2) Maximum power value is 2075.5 кВт (t=0.003 c)

3) Average radial value

# # RT3

**Table E-3.2. Radial energy characteristics of fuel rod # RT3***

| Parameters** | Coordinates of fuel radial layers (mm) | | | |
|---|---|---|---|---|
| | 1 layer (1.23-2.82) | 2 layer (2.82-3.44) | 3 layer (3.44-3.71) | 4 layer (3.71-3.795) |
| Number of fissions $x10^{-14}$ (fiss) | 4.417 | 2.893 | 1.730 | 0.848 |
| Fission density $x10^{-13}$ (fiss/g fuel) | 2.192 | 2.357 | 2.896 | 4.358 |
| Power*** (kW) | 920.8 | 605.2 | 366.6 | 182.5 |
| Energy deposition (cal/g fuel) | 149.8 | 161.5 | 198.7 | 299.2 |
| Energy deposition (J/g fuel) | 627.4 | 676.0 | 832.0 | 1253 |
| Energy deposition**** (per-unit) | 0.501 | 0.540 | 0.664 | 1.000 |

* Average values were determined in accordance with results of RRC KI and VNIIEF calculations

** All parameters were determined for the undamaged section of a fuel stack (see Table C.2)

*** The power for the entire length of each layer at time 0.003 s

**** Energy deposition in current layer/energy deposition in $4^{th}$ layer

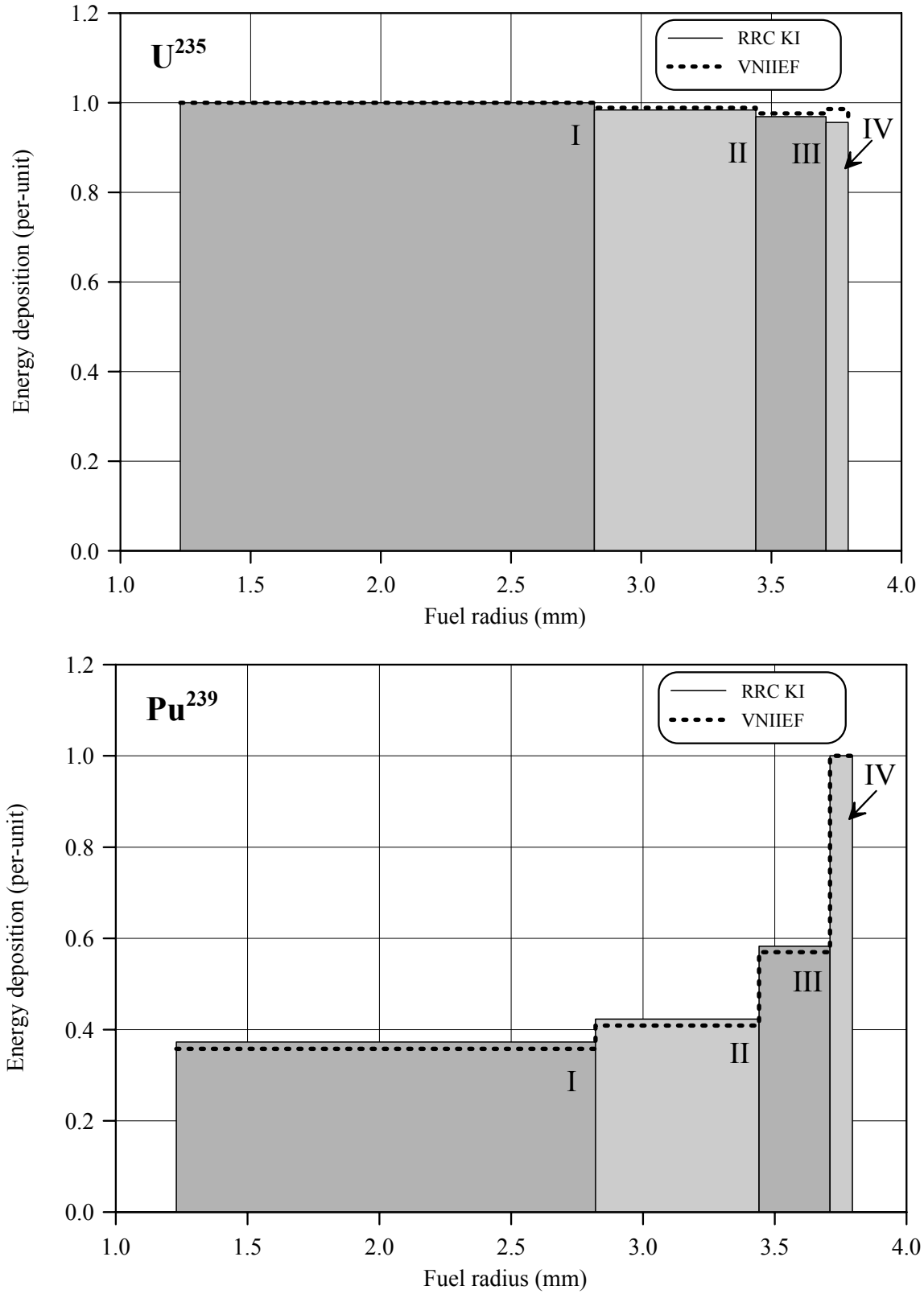


**Fig.E-3.4. $U^{235}$ and $Pu^{239}$ radial distribution of energy deposition for fuel rod # RT3**

# # RT3

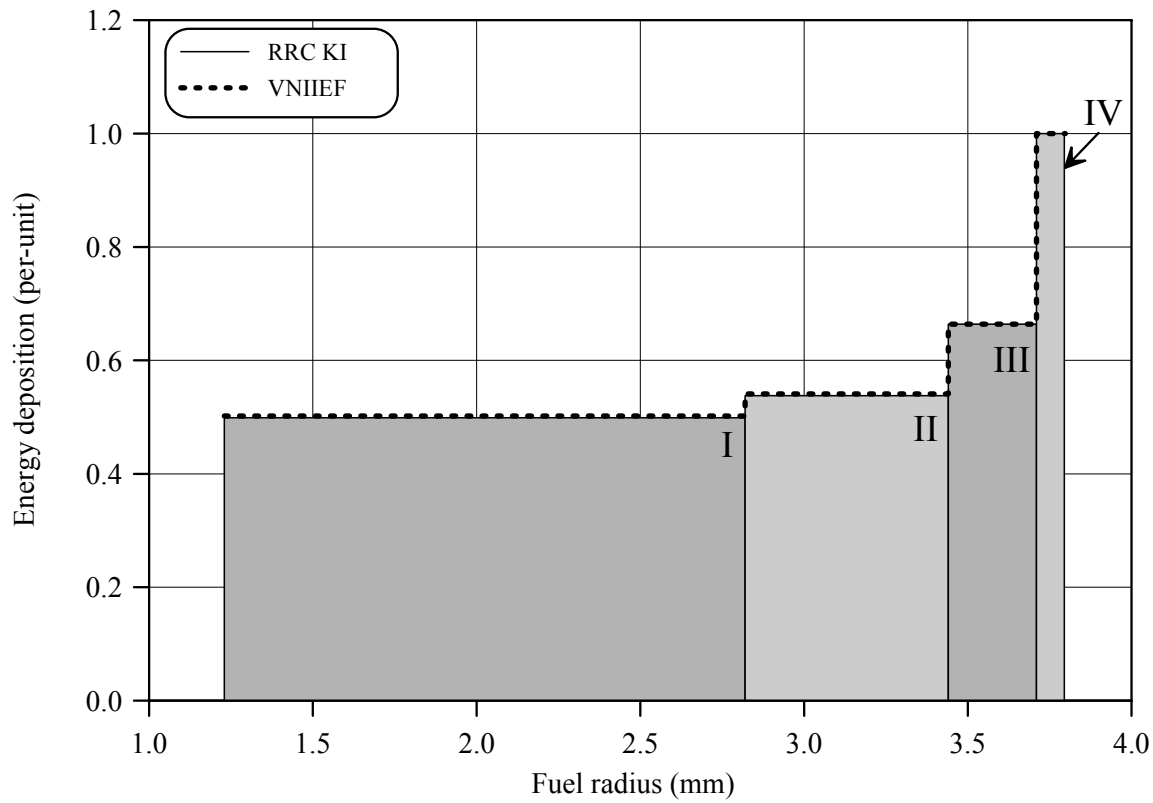


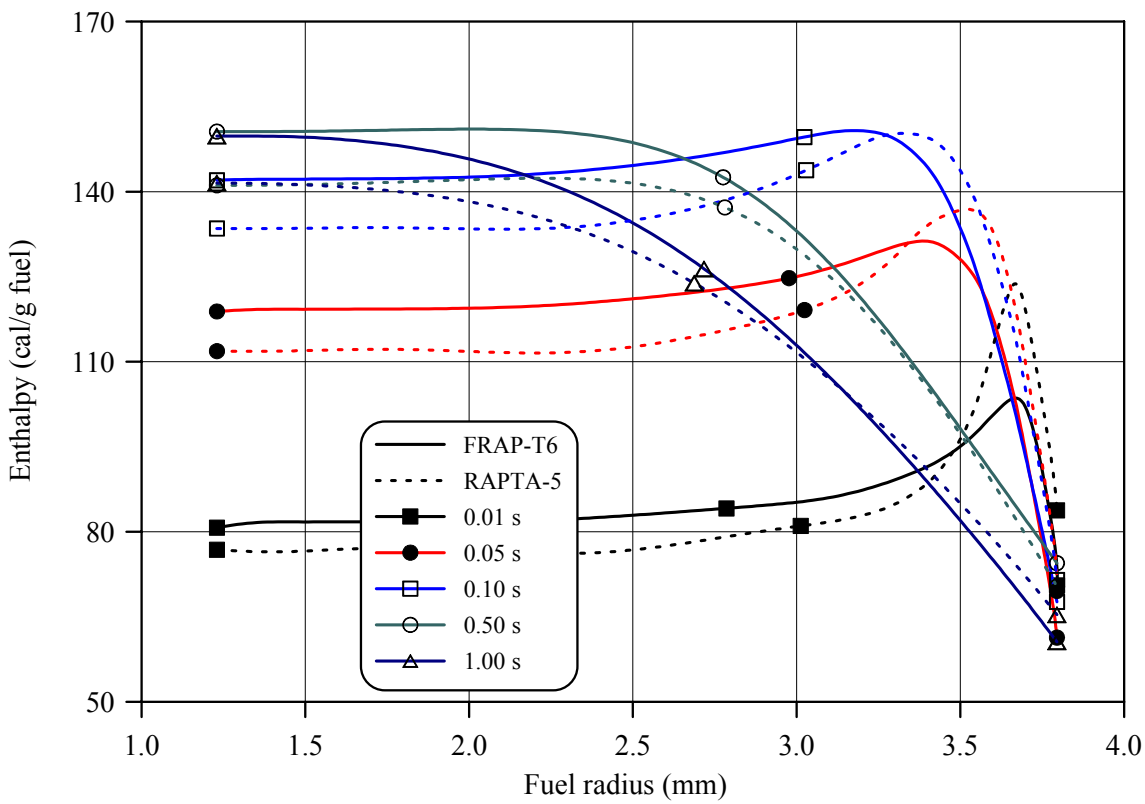


**Fig.E-3.5. Radial distribution of energy deposition and fuel enthalpy for fuel rod # RT3**

# # RT3

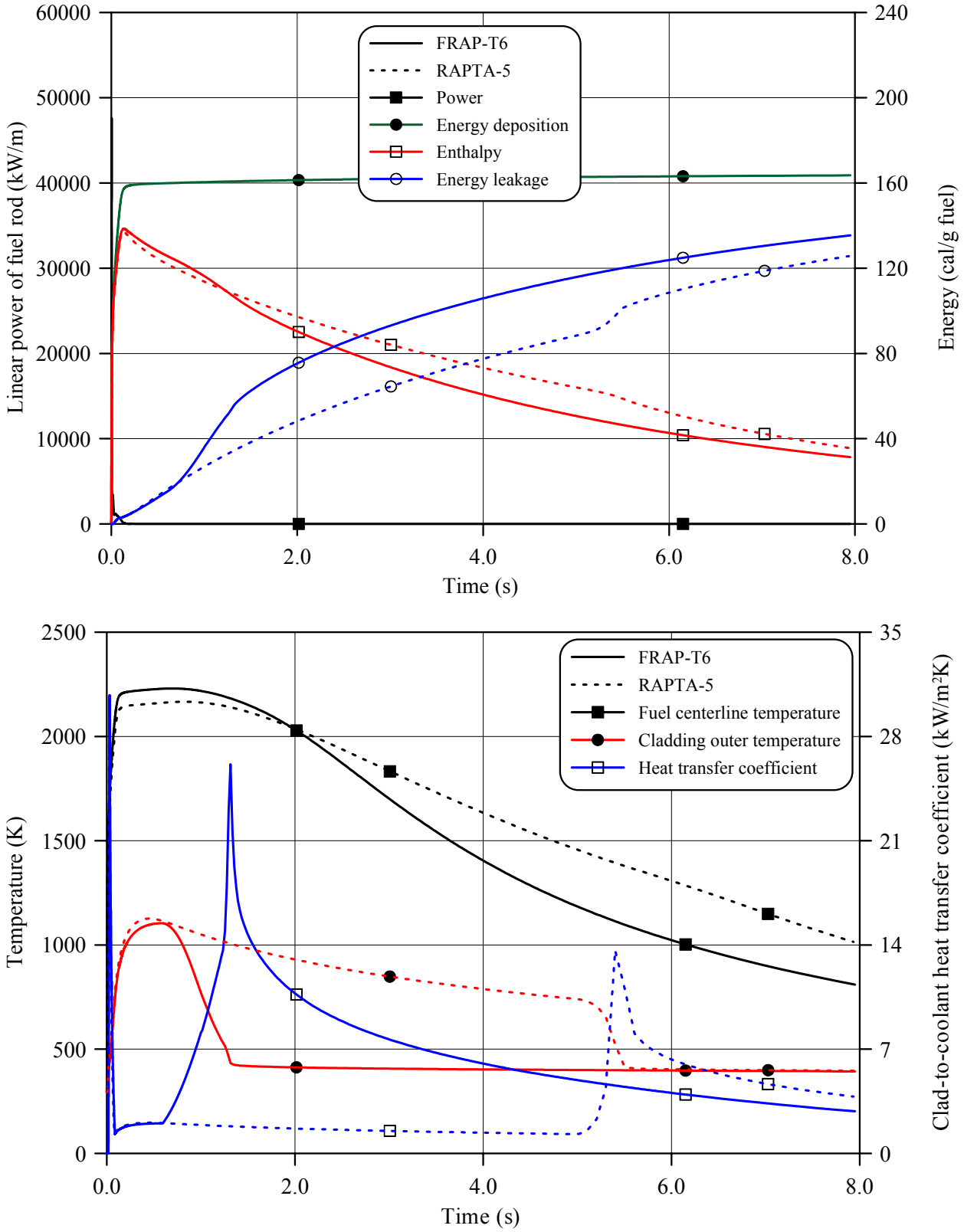


**Fig.E-3.6. Thermal history of fuel rod # RT3 during the BIGR test in accordance with FRAP-T6/VVER and RAPTA-5 calculations**

# # RT3

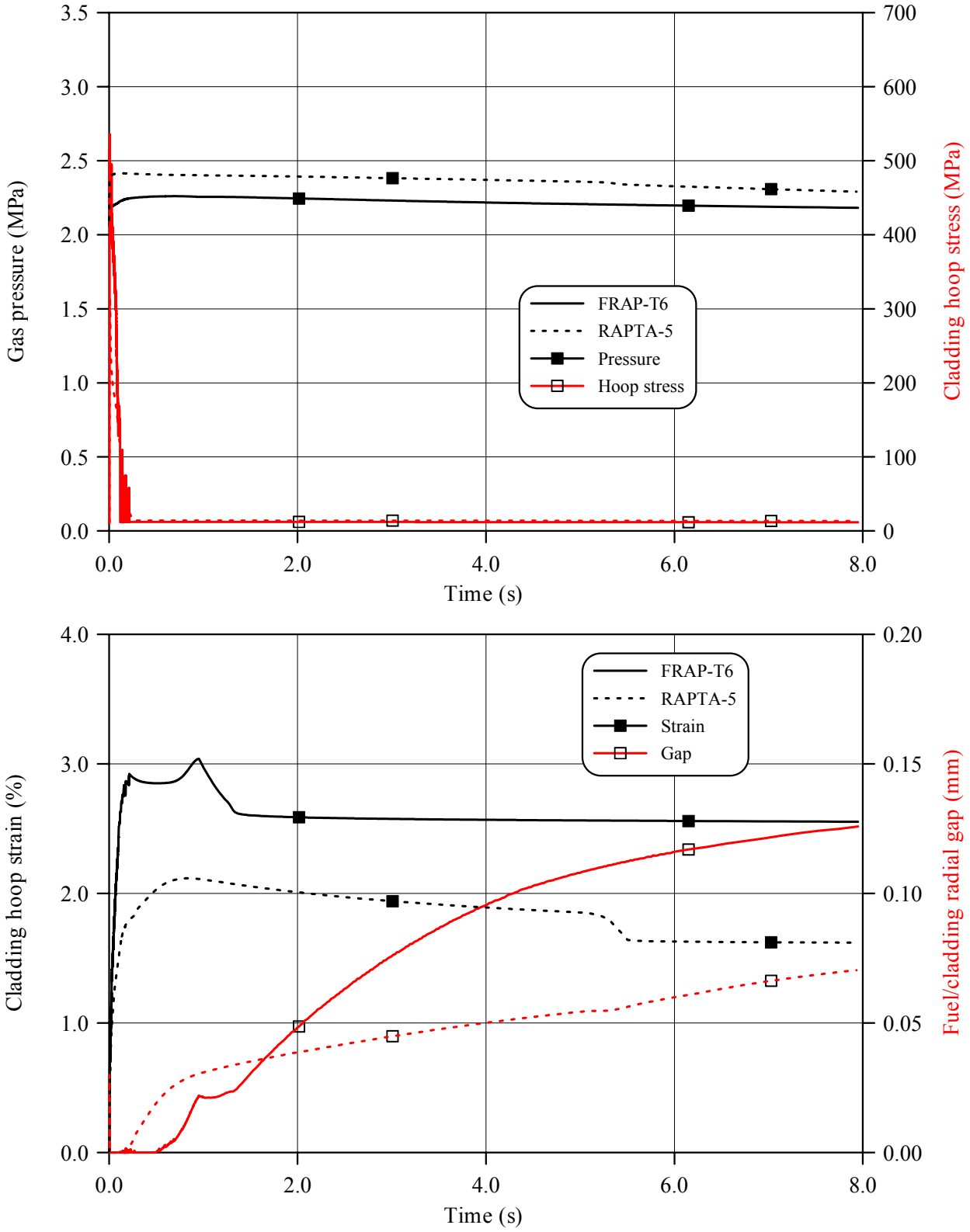


**Fig.E-3.7. Mechanical behavior of fuel rod # RT3 during the BIGR test in accordance with FRAP-T6/VVER and RAPTA-5 calculations**

# # RT3

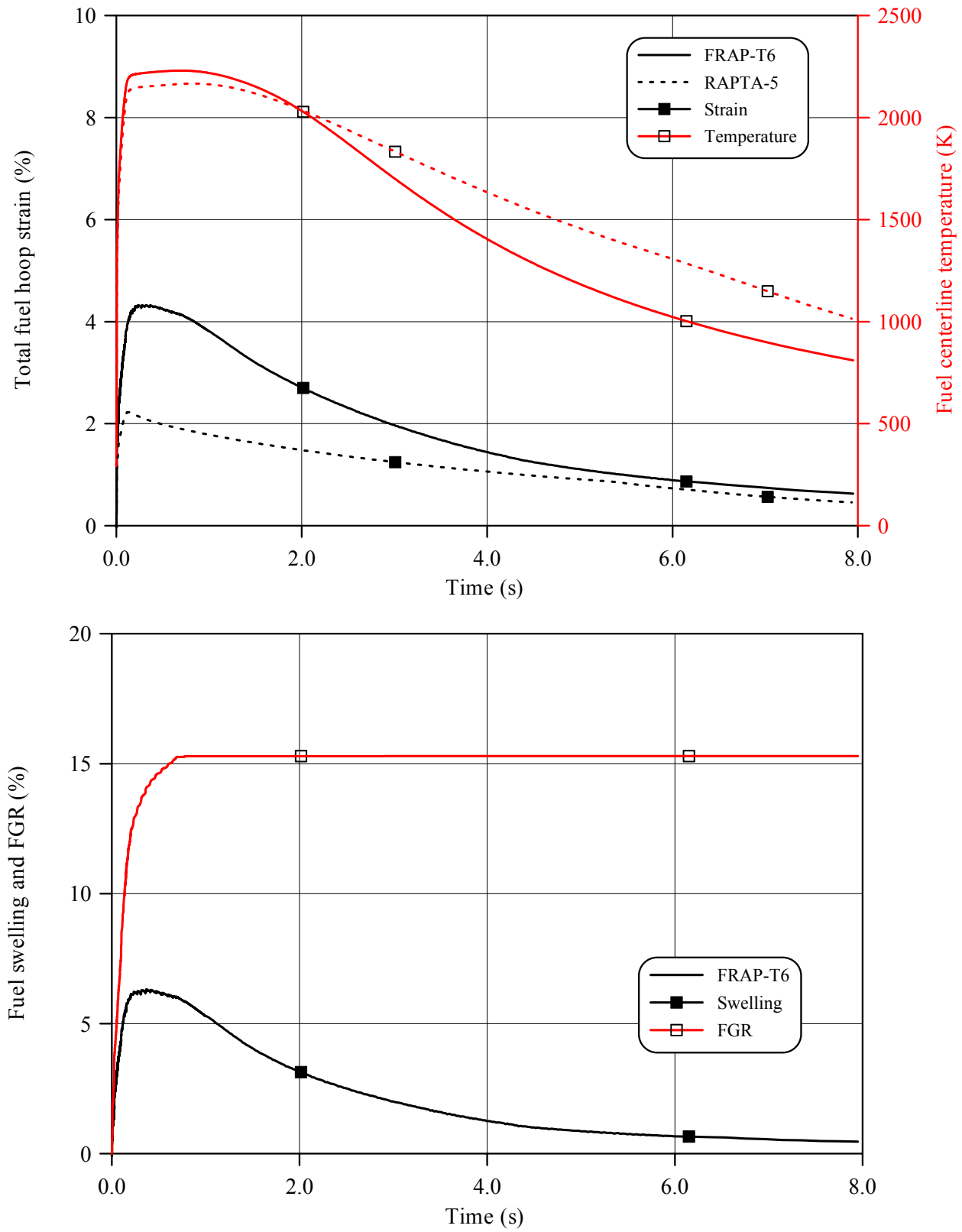


**Fig.E-3.8. Fuel behavior during the BIGR test of fuel rod # RT3 in accordance with FRAP-T6/VVER and RAPTA-5 calculations**

# # RT3

**Table E-3.3. Axial distribution of cladding average outer diameter in fuel rod # RT3***

| Axial coordinate (mm) | Cladding diameter (mm) | Axial coordinate (mm) | Cladding diameter (mm) | Axial coordinate (mm) | Cladding diameter (mm) | Axial coordinate (mm) | Cladding diameter (mm) |
|---|---|---|---|---|---|---|---|
| 36 | 9.208 | 74 | 9.251 | 112 | 9.293 | 150 | 9.314 |
| 38 | 9.231 | 76 | 9.265 | 114 | 9.286 | 152 | 9.307 |
| 40 | 9.245 | 78 | 9.286 | 116 | 9.267 | 154 | 9.300 |
| 42 | 9.242 | 80 | 9.302 | 118 | 9.235 | 156 | 9.308 |
| 44 | 9.242 | 82 | 9.296 | 120 | 9.245 | 158 | 9.340 |
| 46 | 9.205 | 84 | 9.271 | 122 | 9.260 | 160 | 9.365 |
| 48 | 9.150 | 86 | 9.261 | 124 | 9.259 | 162 | 9.372 |
| 50 | 9.131 | 88 | 9.271 | 126 | 9.252 | 164 | 9.323 |
| 52 | 9.092 | 90 | 9.298 | 128 | 9.227 | 166 | 9.225 |
| 54 | 9.064 | 92 | 9.300 | 130 | 9.226 | 168 | 9.129 |
| 56 | 9.059 | 94 | 9.270 | 132 | 9.269 | 170 | 9.070 |
| 58 | 9.058 | 96 | 9.237 | 134 | 9.316 | 172 | 9.052 |
| 60 | 9.059 | 98 | 9.255 | 136 | 9.328 | 174 | 9.051 |
| 62 | 9.073 | 100 | 9.278 | 138 | 9.292 | 176 | 9.045 |
| 64 | 9.137 | 102 | 9.308 | 140 | 9.252 | 178 | 9.409 |
| 66 | 9.198 | 104 | 9.303 | 142 | 9.241 | 180 | 8.521 |
| 68 | 9.251 | 106 | 9.278 | 144 | 9.272 | | |
| 70 | 9.260 | 108 | 9.270 | 146 | 9.298 | | |
| 72 | 9.253 | 110 | 9.281 | 148 | 9.314 | | |

* Measured value determined on the basis of profilometry data (16 azimuthal directions)

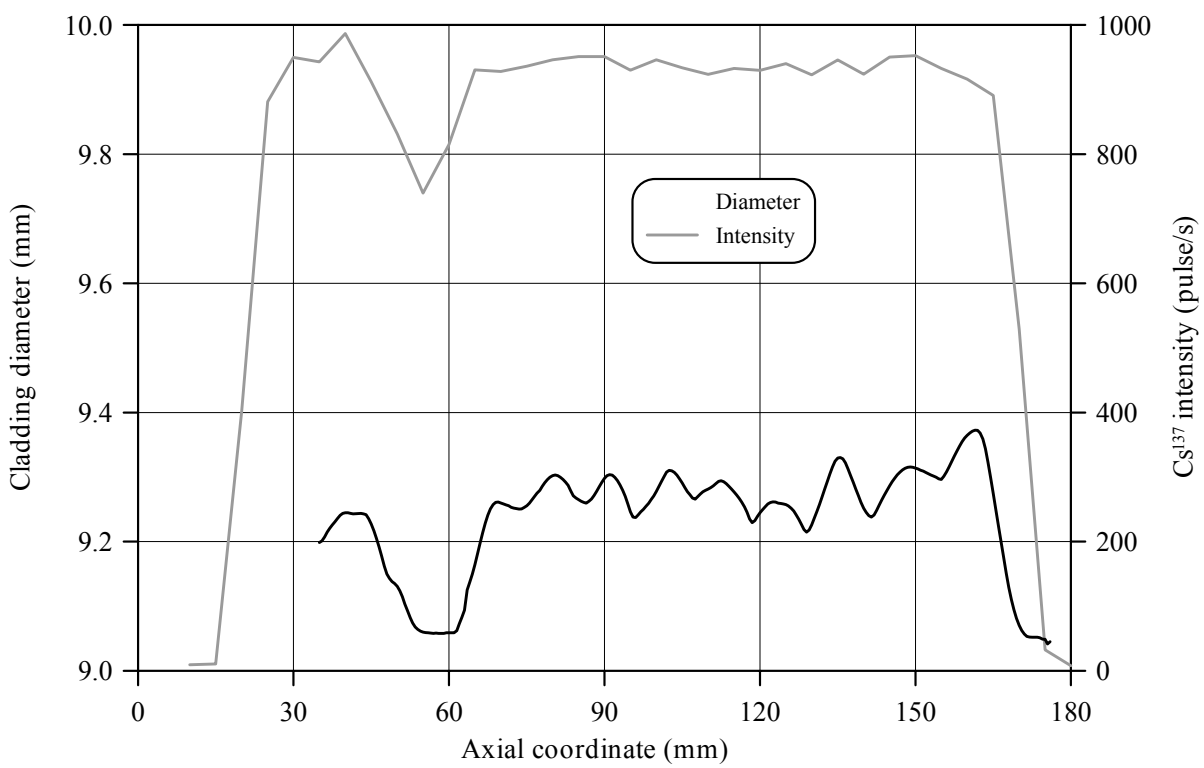


**Fig.E-3.9. Cladding measured average diameter and γ-scanning results for fuel rod # RT3**

**Table E-3.4. The PIE results for fuel rod # RT3**

| | Parameter | Value |
|---|---|---|
| 1. | Cladding outer diameter (mm): | |
| 1.1. | Maximum diameter of the bidimensional data sample in "fuel rod length - azimuthal angle" coordinates (mm) | 9.47 |
| 1.2. | Averaged azimuthal diameter and maximum diameter along the length selected from the sample of averaged azimuthal diameter (mm) | 9.37 |
| 1.3. | Averaged diameter of the bidimensional data sample in "fuel rod length - azimuthal angle" coordinates (mm) | 9.24 |
| 2. | Cladding maximum residual hoop strain (%) | 3.40 |
| 3. | Fuel pellet conditional diameter (mm) in cross-section*: | |
| | at 113 mm elevation | 7.71 |
| 4. | $ZrO_2$ outer thickness (μm) in cross-section: | |
| | at 113 mm elevation | 3–5 |
| 5. | $ZrO_2$ inner thickness (μm) in cross-section: | |
| | at 113 mm elevation | 0 |
| 6. | Parameters characterizing FGR: | |
| 6.1. | Gas composition (% by volume): | |
| | He | 84.76 |
| | $N_2$ | 0.91 |
| | $O_2$ | 0.17 |
| | Ar | 0.015 |
| | $CO_2$ | 0.010 |
| | Kr | 1.28 |
| | Xe | 12.85 |
| 6.2. | Free gas volume ($cm^3$) | 6.1 |
| 6.3. | Gas volume under normal conditions ($cm^3$) | 143.5 |
| 6.4. | Gas pressure under normal conditions (MPa) | 2.35 |
| 6.5. | FGR (%) | 21.30 |

* Reference value determined by the processing of fuel cross-section photographs

# # RT3

**Table E-3.5. Organized BIGR test results for fuel rod # RT3**

| Parameter | | Unit | Value | | |
|---|---|---|---|---|---|
| | | | Measured | Calculated | |
| | | | | FRAP-T6 | RAPTA-5 |
| 1. | Fuel burnup | MW d/kg U | 47.5 | 47.5 | 47.5 |
| 2. | Initial gas pressure | MPa | 2.1 | 2.1 | 2.1 |
| 3. | Energy deposition | cal/g fuel | 167.9 | 167.9 | 167.9 |
| 4. | Peak fuel enthalpy* | cal/g fuel | - | 138.6 | 137.2 |
| 5. | Fuel maximum temperature | K | - | 2266 | 2279 |
| 6. | Maximum temperature of cladding outer surface | K | - | 1104 | 1127 |
| 7. | Cladding burst | Failed, Unfailed | Unfailed | Unfailed | Unfailed |
| 8. | Cladding residual hoop strain** | % | 2.00 | 2.46 | 1.55 |
| 9. | Kr volume content in gas composition after the BIGR test | % | 1.28 | 0.56 | - |
| 10. | Xe volume content in gas composition after the BIGR test | % | 12.85 | 3.37 | - |

* Average value of peak fuel enthalpy is 137.9 cal/g fuel

** Average value along the fuel stack length

# *Appendix E–4*

# *Individual Characteristics of Fuel Rod # RT4 after the BIGR Test*

# # RT4

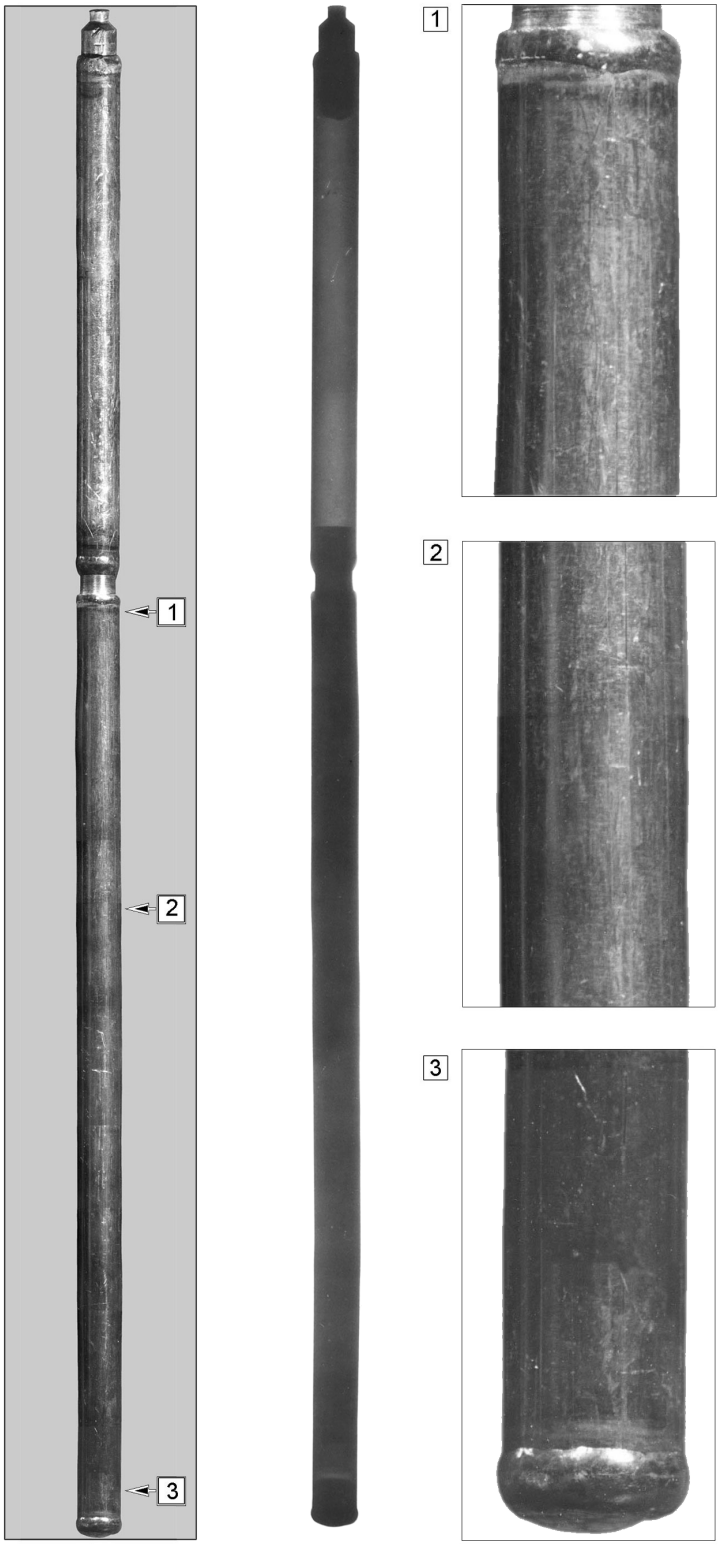


**Fig.E-4.1. Appearance of unfailed fuel rod # RT4 after the BIGR test (photographs and X-ray photograph)**